

Late Quaternary sediments from deep-sea sediment drifts on the Antarctic Peninsula Pacific margin: Climatic control on provenance of minerals

Alessandra Venuti,¹ Fabio Florindo,¹ Andrea Caburlotto,² Mark W. Hounslow,³ Claus-Dieter Hillenbrand,⁴ Eleonora Strada,^{1,5} Franco M. Talarico,⁵ and Andrea Cavallo¹

Received 28 August 2010; revised 15 March 2011; accepted 29 March 2011; published 21 June 2011.

[1] We present results of detailed paleomagnetic investigations on deep-sea cores from sediment drifts located along the Pacific continental margin of the Antarctic Peninsula. High-resolution magnetic measurements on u channel samples provide detailed age models for three cores collected from drift 7, which document an age of 122 ka for the oldest sediments recovered near the drift crest at site SED-07 and a high sedimentation rate (11 cm/kyr) at site SED-12 located close to the Alexander Channel system. Low- and high-temperature magnetic measurements in conjunction with microscopic and mineralogic observations from drifts 4, 5 and 7 indicate that pseudosingle-domain detrital titanomagnetite (partially oxidized and with limited Ti substitution) is the dominant magnetic mineral in the drift sediments. The titanomagnetite occurs in two magnetic forms: (1) a low-coercivity form similar to laboratory-synthesized titanomagnetite and (2) a high-coercivity form ($B_{cr} > 60$ mT). These two forms vary in amount and stratigraphic distribution across the drifts. We did not find evidence for diagenetic magnetic iron sulfides as has been previously suggested for these drift deposits. The observed change of magnetic mineralogy in sediments deposited during Heinrich events on drift 7 appears to be related to warming periods, which temporarily modified the normal glacial transport pathways of glaciogenic detritus to and along the continental rise and thus resulted in deposition of sediments with a different provenance. Understanding this sediment provenance delivery signature at a wider spatial scale should provide information about ice sheet dynamics in West Antarctica over the last ~100 kyr.

Citation: Venuti, A., F. Florindo, A. Caburlotto, M. W. Hounslow, C.-D. Hillenbrand, E. Strada, F. M. Talarico, and A. Cavallo (2011), Late Quaternary sediments from deep-sea sediment drifts on the Antarctic Peninsula Pacific margin: Climatic control on provenance of minerals, *J. Geophys. Res.*, 116, B06104, doi:10.1029/2010JB007952.

1. Introduction

[2] A system of twelve giant deep-sea sediment drifts that are separated by large channels, eroded by turbidity currents, characterizes the continental rise west of the Antarctic Peninsula (Figure 1). These drifts provide the most proximal continuous sedimentary records of late Neogene to Quaternary ice sheet dynamics in this part of West Antarctica [Barker *et al.*, 1999a, 2002]. The sediment drifts are up to 300 km long, 100 km wide and 1 km thick, with the main axis elongated perpendicular to the continental margin [e.g., Rebesco *et al.*, 1996, 1997, 2002, 2007,

Barker *et al.*, 1999b; Amblas *et al.*, 2006; Uenzelmann-Neben, 2006]. The drifts are part of a complex glacial sedimentary feeder dispersal system that is composed of lobes and troughs on the outer shelf, a steep continental slope and deep-sea channels that separate the drifts on the upper rise [e.g., Rebesco *et al.*, 1998; Hernández-Molina *et al.*, 2006].

[3] During the 1990s, these drifts were intensely investigated by the SEDANO program (Sediment Drift of the Antarctic Offshore) of the Italian Programma Nazionale di Ricerche in Antartide (PNRA), the British Antarctic Survey (BAS), and by Ocean Drilling Program (ODP) Leg 178 [Barker *et al.*, 1999a, 2002]. During two SEDANO cruises with the R/V *OGS-Explora* (1995/1997–98), seismic surveys, gravity coring, and moorings with current meters and sediment traps yielded information about the morphology and mechanisms of deposition along the Pacific continental margin [e.g., Camerlenghi *et al.*, 1997a, 1997b; Rebesco *et al.*, 1997, 2002, 2007; Pudsey and Camerlenghi, 1998; Harland and Pudsey, 1999; Lucchi *et al.*, 2002; Giorgetti *et al.*,

¹Istituto Nazionale di Geofisica e Vulcanologia, Rome, Italy.

²Istituto Nazionale di Oceanografia e di Geofisica Sperimentale, Sgonico, Italy.

³Lancaster Environment Centre, Lancaster University, Lancaster, UK.

⁴British Antarctic Survey, Cambridge, UK.

⁵Dipartimento di Scienze della Terra, Università di Siena, Siena, Italy.

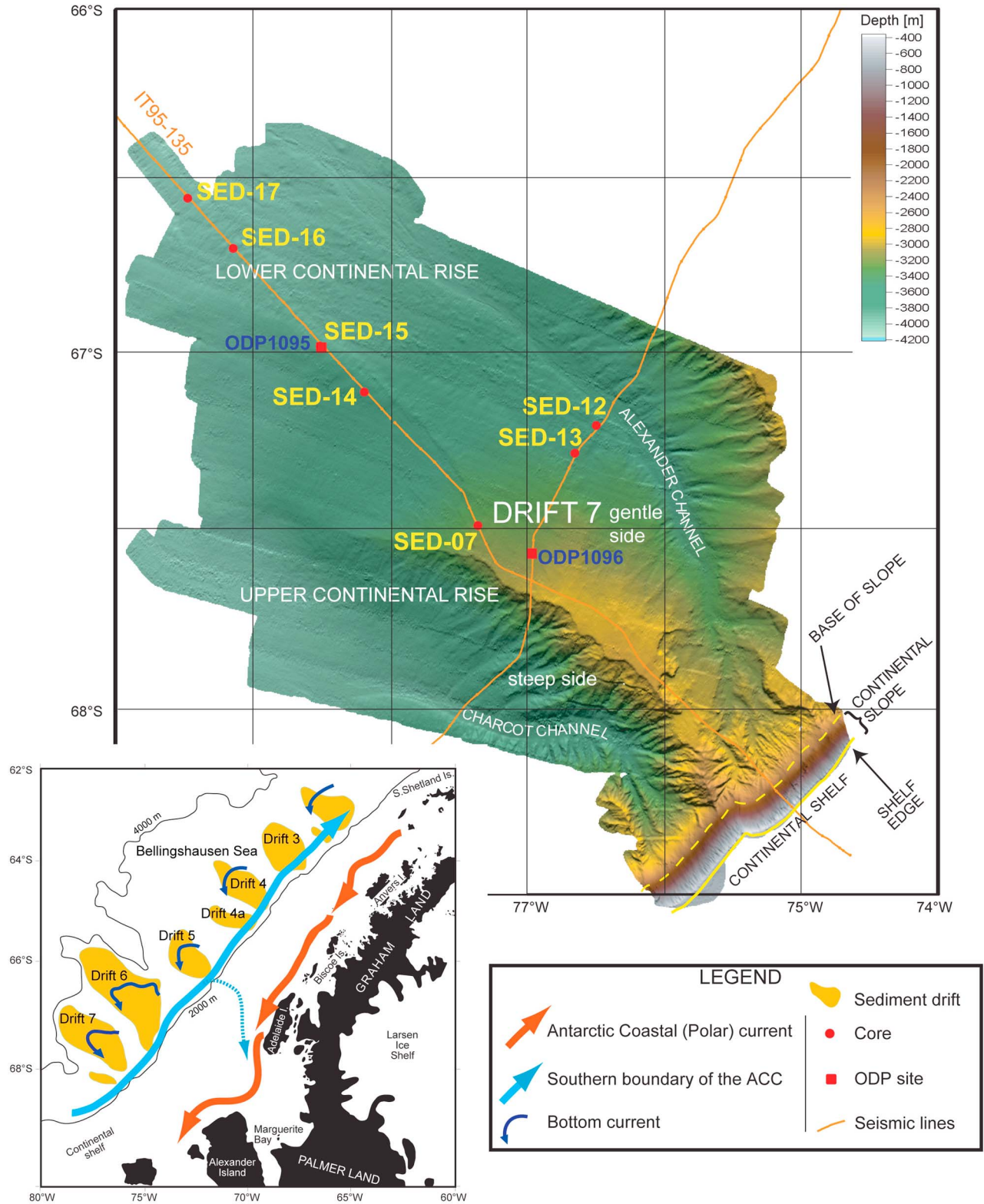


Figure 1. Color-shaded relief bathymetric map of sediment drift 7 off the Antarctic Peninsula Pacific margin with location of SEDANO gravity cores (mentioned in the text) and ODP Leg 178 drill sites. The inset is a schematic of the present-day surface and bottom water circulation along the western margin of the Antarctic Peninsula. The hatched blue arrow illustrates episodic intrusion of Circumpolar Deep Water onto the shelf [Hillenbrand *et al.*, 2008a, and references therein].

2003; Villa *et al.*, 2003; Lucchi and Rebesco, 2007]. The SEDANO program collected 17 gravity cores from drift 7 and an additional two cores at drift 4 [Lucchi *et al.*, 2002], while BAS recovered 11 piston cores from the drifts located to the NE of drift 7 on cruise JR19 with RRS *James Clark Ross* [Pudsey, 2000].

[4] Paleomagnetic and mineral magnetic studies were conducted by Sagnotti *et al.* [2001] and Macri *et al.* [2006] on seven gravity cores (SED-02, SED-04, SED-06, SED-14, SED-15, SED-16, and SED-17) collected on drift 7 (Figure 1). The ages of these sequences were determined using relative paleomagnetic intensity (RPI) [Sagnotti *et al.*, 2001; Macri *et al.*, 2006], with biostratigraphic and chemostratigraphic information providing additional age constraints [Pudsey and Camerlenghi, 1998; Lucchi *et al.*, 2002; Villa *et al.*, 2003]. The RPI-based high-resolution age models established by Sagnotti *et al.* [2001] and Macri *et al.* [2006] suggested a link between the occurrence of intervals with magnetic coercivity minima in drift 7 and the simultaneous deposition of layers rich in iceberg-rafted debris (IRD) in the North Atlantic (so-called “Heinrich layers” [e.g., Heinrich, 1988; Hemming, 2004]) during major rapid cooling events between ~12 kyr and ~60 kyr ago. In cores from drift 7, a variable mixture of detrital pseudosingle-domain (PSD) magnetite (Fe_3O_4) and fine-grained monoclinic pyrrhotite (Fe_7S_8) was inferred by Sagnotti *et al.* [2001], with magnetite being the main magnetic mineral [cf. Macri *et al.*, 2006]. Contrary to this mineralogical interpretation, Hawkes *et al.* [2003] identified in sediment cores from drifts 3, 4, 4a and 5 only magnetite. Understanding the magnetic mineral responsible for the remanence is important because diagenetic formation of an iron sulfide component may have delayed the magnetic field recording process to some time after deposition [e.g., Florindo and Sagnotti, 1995; Roberts *et al.*, 2005; Sagnotti *et al.*, 2005; Florindo *et al.*, 2007; Roberts *et al.*, 2010].

[5] The main objectives of our study are to (1) provide robust identification of the main magnetic minerals in the drift sediments, which is important for understanding the paleomagnetic recording process, and (2) construct a robust chronostratigraphic framework for cores SED-7, SED-12, and SED-13, which is important for reconstructing Late Pleistocene paleoenvironments of the Antarctic Peninsula. The Antarctic Peninsula may represent the best natural laboratory to investigate the interaction of atmosphere, hydrosphere and cryosphere and the response of Earth's climate system to rapid regional warming [e.g., Florindo and Siegert, 2008]. Over the past 50 years, the Antarctic Peninsula has experienced the greatest atmospheric temperature increase on Earth, rising by nearly 3°C [e.g., King *et al.*, 2003; Turner *et al.*, 2005], which is approximately 10 times the mean rate of present global warming [Intergovernmental Panel on Climate Change (IPCC), 2007].

[6] We have investigated the paleomagnetic properties of two gravity cores (SED-12 and SED-13) located near the Alexander Channel system and two cores (SED-07 and SED-14) located near the crest of drift 7 (Figure 1). We also examined the spatial distribution of magnetic minerals in the drift 7 sediments, and compared these results to the mag-

netic mineralogy in sediments recovered from drifts 4 and 5 located to the NE of drift 7.

2. Oceanographic Setting, Site Locations, and Core Lithostratigraphy

[7] The Pacific continental margin of the Antarctic Peninsula is under the influence of the Southern Boundary (SB) of the Antarctic Circumpolar Current (ACC), which is a massive eastward flowing wind-driven current. The ACC plays an important role in the thermohaline circulation and heat budget of the world ocean (Figure 1) [e.g., Barker *et al.*, 2007; Carter *et al.*, 2008]. Surface and deep-water masses north of the SB are located within the Antarctic Zone, i.e., within the clockwise flowing ACC. Nevertheless, Hillenbrand *et al.* [2008a] showed that in the area of investigation the ACC only affects ocean circulation above about 1000 m water depth, whereas today, and for most of the late Neogene and Quaternary, a generally southwestward flowing bottom current affected deposition on the drifts (Figure 1). Surface water currents on the continental shelf to the south of our study area are driven by the westward flowing Antarctic Coastal (or Polar) Current, where the direction of flow is mainly controlled by the orientation and shape of the Antarctic coast (Figure 1).

[8] The large hemipelagic sediment drifts on the Pacific margin of the Antarctic Peninsula are characterized by an asymmetric cross section, with a steep southwestern side and a gently sloping northeastern side (Figure 1). Based on both multichannel seismic profiles [Rebesco *et al.*, 1996, 1997, 2007] and core analysis [Pudsey and Camerlenghi, 1998; Pudsey, 2000; Lucchi *et al.*, 2002; Hillenbrand and Ehrmann, 2005], this geometry is interpreted to result from the interplay between turbidity and bottom currents: fine-grained particles supplied by turbidity currents running through the channels spill over the channel banks (in particular the western banks), and are entrained in the SW flowing bottom contour currents and so are redeposited over the continental rise, thereby contributing to the growth of interchannel sediment drifts [e.g., Rebesco *et al.*, 2007]. The sedimentary successions in cores from the gentle NE slope of drift 7 facing the Alexander Channel system (Figure 1) were therefore directly influenced by both turbidity and contour currents [Lucchi *et al.*, 2002].

[9] Up to nine lithostratigraphic units, named A to I, have been identified within the mid to late Pleistocene successions of drifts 1 to 7 [Pudsey and Camerlenghi, 1998; Pudsey, 2000; Lucchi *et al.*, 2002]. The lithostratigraphic units were correlated by magnetic susceptibility profiles, clay mineral assemblages, sediment facies and textural characteristics, and were assigned to marine isotope stages (MIS) 1 to 11 on the basis of biostratigraphy, chemostratigraphy and excess ^{230}Th activity [Pudsey and Camerlenghi, 1998; Pudsey, 2000; Lucchi *et al.*, 2002; Villa *et al.*, 2003]. Interglacial units consist of brown bioturbated hemipelagic muds with microfossils (diatoms, foraminifera, radiolaria, calcareous nannofossils) and ice-rafted debris (IRD), while glacial units consist of olive gray to gray, laminated terrigenous muds [Pudsey and Camerlenghi, 1998; Pudsey, 2000; Lucchi *et al.*, 2002; Villa *et al.*, 2003]. Tephra layers with a trachytic composition occur within lithostratigraphic units D and C (latest MIS 6 and early MIS 5) [Pudsey and Camerlenghi,

Table 1. Location of the Studied Sediment Cores

Core	Latitude (°S)	Longitude (°W)	Water Depth (m)	Core Length (m)
SED-7	67°29.30'	77°21.05'	3266	5.79
SED-12	67°12.48'	76°29.45'	3620	6.97
SED-13	67°17.16'	76°38.80'	3559	6.67
SED-14	67°06.82'	78°10.48'	3768	6.98
PC102	64°35.2'	69°24.8	2787	9.4
PC107	65°54.0'	72°39.9'	3080	8.4
PC108	65°42.0'	73°38.1'	3601	9.2
PC111	64°19.0'	70°26.2	3357	11.1

1998; Pudsey, 2000; Lucchi *et al.*, 2002], and provide important time markers for correlating and dating cores from the West Antarctic continental margin [Hillenbrand *et al.*, 2008b].

3. Material and Methods

[10] From the original set of 17 gravity cores from drift 7, which were collected during the SEDANO-I and -II projects, we selected four cores (SED-07, SED-12, SED-13, and SED-14) for paleomagnetic and magnetic mineralogy investigations. These cores were collected near the crest of drift 7 and in the proximity of the Alexander Channel system, respectively (Figure 1 and Table 1). The sediment cores do not have sharp boundaries between different lithological units, which suggests that major erosion did not affect the recovered sequences [Lucchi *et al.*, 2002]. However, lithostratigraphic Unit A (corresponding to MIS 1) is missing in both cores SED-12 and SED-14 and appears to be condensed in core SED-07, which suggests that, at least during the Holocene, erosive, current-induced winnowing, or nondeposition played an important role at these sites. Alternatively, Unit A may have been lost or only partially recovered at these sites during coring operations [Lucchi *et al.*, 2002]. The cores were logged for magnetic susceptibility using a Bartington Instruments MS2F point sensor on split cores [Pudsey and Camerlenghi, 1998] and a Bartington Instruments MS2C loop sensor on the whole core [Lucchi *et al.*, 2002].

[11] A suite of mineral magnetic measurements was also carried out on BAS piston cores PC102 and PC111 from drift 4 and PC107 and PC108 from drift 5 (see inset in Figure 1 for location of the drifts and Table 1). Magnetic susceptibility had been measured at 2 cm intervals on the split surface of the archive halves of these cores by Pudsey [2000] and Ó Cofaigh *et al.* [2001], who used a Bartington Instrument susceptibility meter with MS2F point sensor (for a compilation of magnetic susceptibility data from the SEDANO and BAS cores, see supplementary information of Hillenbrand *et al.* [2008b]). All metadata for the SEDANO and BAS cores studied here are given as auxiliary material (Table S1 to S7) and in the work of Pudsey [2000] and Lucchi *et al.* [2002].¹

3.1. Sampling

[12] Cores SED-07, SED-12, and SED-13 from drift 7 were sampled using u channels (1.2 m in length) at the core

repository of the Italian Museo Nazionale dell'Antartide in Trieste (u channels are open-sided 2 cm × 2 cm square cross-sectioned liners made of nonmagnetic plastic [Weeks *et al.*, 1993]). After removing the sediment-filled u channel from the core, an airtight cover was clipped over the u channel to hold the sediment in place and to prevent it from drying. The u channel ends were sealed using plastic film and tape to minimize moisture loss. The u channels were taken from the center of the archive halves of cores SED-7 and SED-13 and from the working halves of core SED-12 and the working half of one section of core SED-14. This section of core SED-14 was sampled to investigate the anomalous inclination values of the characteristic remanent magnetization (ChRM) observed on the corresponding archive half [Macri *et al.*, 2006].

[13] A suite of mineral magnetic measurements was carried out on sediment samples from lithostratigraphic units A to C in cores PC102 and PC111 from drift 4 and cores PC107 and PC108 from drift 5. Discrete samples for magnetic analyses were collected by inserting ~10 cm³ plastic boxes into the sediment, and sealing the resulting samples.

3.2. Magnetic Analyses

[14] All magnetic analyses on the SEDANO cores were performed at the paleomagnetism laboratory of the Istituto Nazionale di Geofisica e Vulcanologia (INGV) in Rome. Natural and artificial magnetizations were measured using a narrow access pass through 2-G Enterprises cryogenic magnetometer (model 755R) with an internal diameter of 4.2 cm [Weeks *et al.*, 1993], equipped with three DC SQUID sensors (noise level 3×10^{-9} Am²kg⁻¹), housed in a Lodestar Magnetics shielded room. The natural remanent magnetization (NRM) was measured at 1 cm intervals, although smoothing occurs due to the Gaussian shape of the response curve of the magnetometer pickup coils [Weeks *et al.*, 1993] (the half power width suggests smoothing across 4.8 cm for the radial X and Y directions and 5.9 cm for the axial Z direction). Data from the upper and lower 5 cm of each u channel were not used, because these data are affected by “edge effects” due to the width of the magnetometer response function. The NRM was then stepwise demagnetized using an in-line static demagnetizer at peak alternating fields (AF) of 10, 20, 30, 40, 50, 60, 80, and 100 milliTesla (mT), with measurements after each step. The ChRM directions and the maximum angular deviation (MAD) [Kirschvink, 1980] were computed using the software of Mazaud [2005]. The studied cores lack azimuthal orientation. The geocentric axial dipole field at the latitude of the coring sites (about 67°S; Table 1) has an inclination of -78°.

[15] After demagnetization of the NRM, mineral magnetic analyses were carried out on both u channel and discrete samples. Low-field volume specific magnetic susceptibility (κ) was measured at 1 cm intervals using a Bartington Instruments MS2C loop sensor (frequency of 0.565 kHz) with 40 mm diameter, mounted in line with the 2-G Enterprises magnetometer system. An anhysteretic remanent magnetization (ARM) was imparted using a solenoid that is mounted in-line with the demagnetization coils on the INGV magnetometer system (a DC bias field of 0.1 mT was used in conjunction with a peak AF of 100 mT) and was then measured at 1 cm intervals.

¹Auxiliary materials are available at <ftp://ftp.agu.org/apend/jb/2010/jb007952>.

[16] Additional mineral magnetic analyses were carried out on discrete samples (<50 mg) collected from the u channels of the drift 7 cores. Isothermal remanent magnetization (IRM) acquisition curves, in 16 steps up to 0.5 T, and hysteresis properties, were determined using an alternating gradient magnetometer (AGM) (Princeton Measurements Corporation Model 2900 Micromag). The hysteresis parameters measured include the saturation magnetization (M_s), saturation remanent magnetization (M_{rs}), and coercive force (B_c). Backfield demagnetization of the IRM was used to determine the coercivity of remanence (B_{cr}). The ratios of M_{rs}/M_s and of B_{cr}/B_c are useful indicators of the domain state of magnetic grains, as outlined by *Day et al.* [1977].

[17] First-order reversal curve (FORC) measurements [Roberts et al., 2000] were made using a vibrating sample magnetometer (VSM, Princeton Measurements Corporation Model 3900 Micromag) on representative intervals with sufficiently strong magnetizations to investigate micro-coercivity and magnetic interaction among magnetic particles. The FORC diagrams were created using the FORCinel software [Harrison and Feinberg, 2008].

[18] Continuously monitored temperature dependence of κ (up to 700°C) was measured using an AGICO CS-3 furnace equipped Kappabridge KLY-3 (noise level 2×10^{-8} SI volume units), both in air and with argon gas flow (to prevent oxidation) in order to identify Curie temperatures of the magnetic minerals [Hrouda, 1994].

[19] All magnetic measurements on the BAS sediment cores recovered from drifts 4 and 5 were carried out at the Centre for Environmental Magnetism and Palaeomagnetism in Lancaster (UK). The mineral magnetic analyses included measurement of low-frequency (χ_{lf}) and high-frequency mass-specific magnetic susceptibility using a Bartington Instruments MS2 meter, ARM acquisition in DC fields of 0.08 mT (80 mT AF field), and backfield DC demagnetization at 20, 50, 100 and 300 mT of a 1 T saturation IRM (SIRM). These remanences were measured on a Minispin fluxgate magnetometer (noise level $\sim 0.5 \times 10^{-8}$ Am²). Orthogonally applied IRMs (using inducing fields of 0.1 T, 0.3 T and 1 T) for selected samples were thermally demagnetized [Lowrie, 1990] to identify unblocking characteristics of different coercivity fractions. This was performed using a Magnetic Measurements thermal demagnetizer, with remanences measured on a CCL three-axis SQUID magnetometer. Thermal unblocking (in zero magnetic field) of a 2.5 T IRM applied at 10 K was measured on a Quantum Design magnetic property measurement system, to examine possible low-temperature magnetic transitions associated with magnetite, titanomagnetite and/or pyrrhotite.

3.3. Microscopic Analyses and Mineral Extraction

[20] Scanning electron microscopy and energy dispersive spectrometry (SEM-EDS) were performed to qualitatively identify opaque minerals in selected samples from glacial and interglacial lithostratigraphic units in drift 7 cores SED-12 (close to the Alexander Channel system) and SED-14 (drift crest). We used a Philips 515 scanning electron microscope with an EDAX 9100/70 X-ray energy dispersive detector, running at 15 kV and with an emission current of 20 nA at the Dipartimento di Scienze della Terra, Università di Siena. Additional analyses were carried out on a set of

resin impregnated polished sections from cores SED-07, SED-12, and SED-14 using a field emission scanning electron microscope (FESEM) operated at 10 kV. In addition, a subset of samples from the same cores was gently ground into a fine powder and magnetic minerals were extracted using a Nd-Fe-B-REE (Rare Earth Element) magnet housed in a plastic sheath. Elemental analyses were performed on individual minerals using a JEOL JSM-6500F thermal FESEM, which is a high performance analytical FESEM that integrates with the JEOL energy dispersive X-ray analyzer.

[21] Magnetic mineral extractions from selected samples taken from the cores recovered on drifts 4 and 5 were performed using both a quick method (~ 0.5 h) of extraction (Me) and the magnetic probe (Mp) method detailed by *Hounslow and Maher* [1999]. The former method tends to limit oxidation of sulfides, but tends to be biased toward extraction of more strongly magnetic particles, often with larger grain sizes. In contrast, the latter method is more representative and removes also the smaller magnetic particles, but the longer extraction times (7 days) tends to oxidize any greigite that may be present [Hounslow and Maher, 1996]. The extracts were then examined optically under transmitted and reflected light at magnifications up to 1000 \times , and were subjected to X-ray diffraction to evaluate their mineralogy. The magnetite lattice spacing was determined with reference to the quartz peaks [e.g., *Hounslow and Maher*, 1999].

3.4. Chronology

[22] Age models were developed for cores SED-12, SED-13, and SED-07 by peak-to-peak correlation of their physical properties with those of the SEDANO cores, that have been dated using RPI correlation [Sagnotti et al., 2001], using the 'linage' function of the AnalySeries 2.0.4.2 software package [Paillard et al., 1996] (see paragraph 4.4 below). We correlated the κ profile of core SED-12 with that of SED-02 and the κ profile of core SED-07 with those of cores SED-04 and SED-06, respectively (for core locations see Figure 1). The ARM/ κ ratio was then used for correlating core SED-13 to core SED-12. In this case, we preferred ARM/ κ rather than the magnetic susceptibility because it displays a clearer correspondence between the two profiles.

4. Results and Interpretation

4.1. Paleomagnetism

[23] The NRM intensity of the studied samples is between 0.1 and 0.2 A/m and is characterized by stable demagnetization behavior with MAD values mostly <5° and never >10°. Typical demagnetization behavior is shown in Figure 2. Most of the studied intervals have a low-stability, steep inclination normal polarity remanence acquired during coring and/or storage that was successfully removed at 10–20 mT. The ChRM was clearly identified as a single, stable and well-defined remanence component above 20 mT for most of the analyzed sediments (Figure 2). For some intervals, samples were not completely demagnetized at a peak AF of 100 mT, which indicates the presence of a high-coercivity magnetic phase. The ChRM inclination record for these cores always indicates normal polarity (negative inclination), but the inclination records have occasional swings to inclinations of about –30° (Figure 3a), possibly

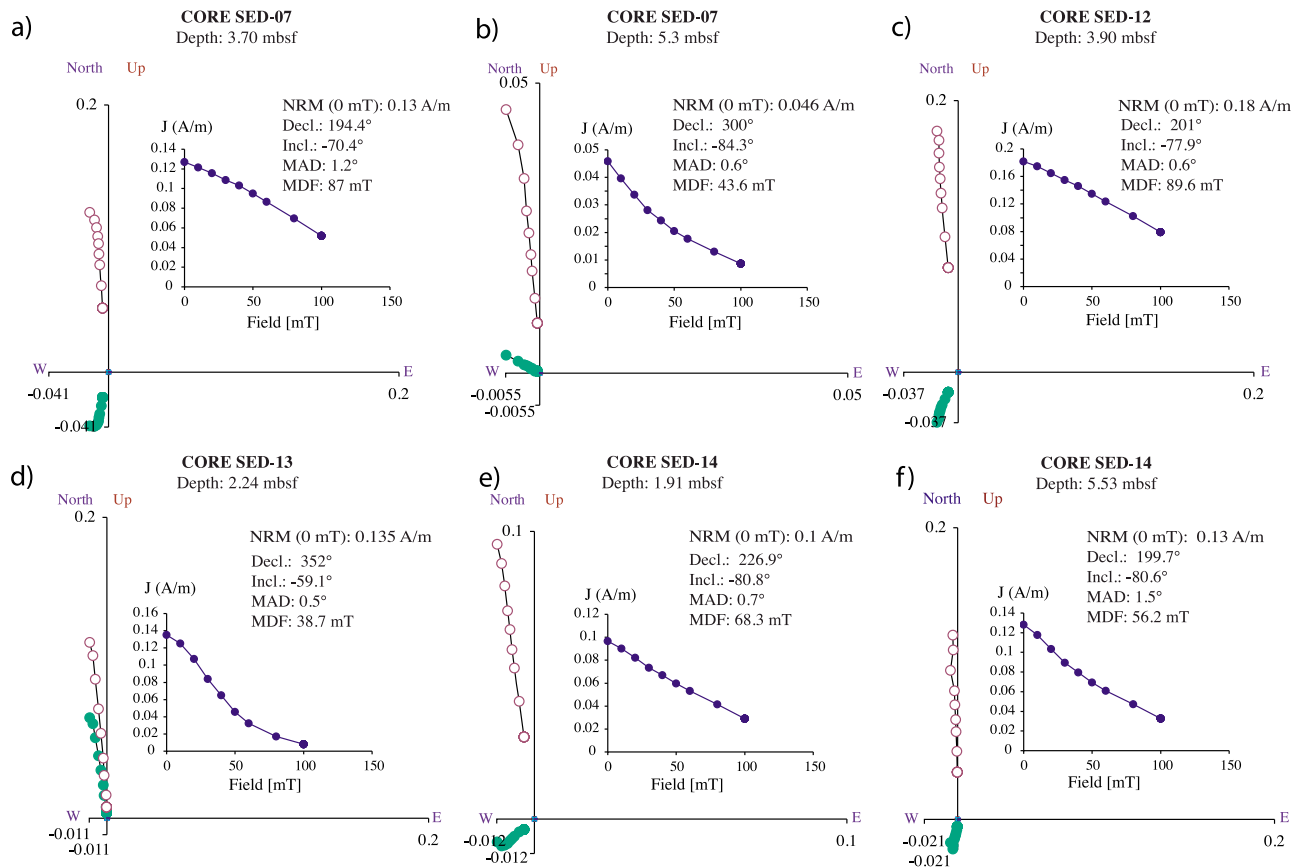


Figure 2. Typical orthogonal vector component diagrams and intensity decay curves for cores SED-07, SED-12, SED-13, and SED-14. (a, c, and f) Samples are from glacial lithostratigraphic units; (b and e) samples from interglacial units; (d) sample from an interval of a glacial unit with a relative minimum of MDF_{NRM} (H2 in Figure 3b). Projections onto the vertical plane are represented by open circles, while projections onto the horizontal plane are denoted by green circles. Decl., declination; Incl., inclination; MAD, maximum angular deviation of the best fit line through the demagnetization data; MDF, median destructive field line, the field at which half of the original magnetization has been demagnetized.

through (1) smoothed recording of geomagnetic excursions caused by postdepositional remanent magnetization (PDRM) acquisition [e.g., Roberts and Winklhofer, 2004], (2) deformation following acquisition of the primary magnetization (e.g., coring deformation [e.g., Acton et al., 2002]), (3) the presence of small and highly magnetic pebbles within the sediment [e.g., Venuti and Florindo, 2004; Florindo et al., 2005]. The latter hypothesis is supported by petrographic analysis on granule- to pebble-sized clasts from these cores, which documents the presence of rhyolite, basalt, cataclastic gabbro, quartzdiorite, volcanoclastic microbreccia with fine-grained biotite-muscovite gneiss and siltstone. Both the occurrence of clasts with highly magnetic petrologies and the effects of granule and pebble contents on magnetic susceptibility records have been previously reported for sediment cores from Antarctic Peninsula drifts [Pudsey and Camerlenghi, 1998; Pudsey, 2000; Ó Cofaigh et al., 2001; Macri et al., 2006; Cowan et al., 2008]. An interval with unusually shallow ChRM inclinations, which Macri et al. [2006] observed between ca 3.1 and 4.1 mbsf in the archive half of core SED-14, is also evident from our measurements on the working half (Figure 3b). Thus, our finding supports the

conclusion of Macri et al. [2006] that the relatively coarse-grained lithology in the corresponding section of core SED-14 is responsible for the shallow ChRM inclinations. We also argue that the shallow inclinations observed in some intervals of the other SEDANO cores (Figure 3a) may be caused by higher contents of larger clasts, which represent the coarse IRD fraction.

4.2. Mineral Magnetic Analyses

4.2.1. Magnetic Mineralogy of Sediments From Drift 7

[24] In the cores from drift 7, variations of concentration-dependent magnetic parameters (κ and ARM) (Figure 3a) remain within about the same order of magnitude (κ ranges between 13 and 135×10^{-5} SI and ARM ranges between 0.1 and 0.8 A/m). The largest variability occurs in silty layers, which are mainly present within glacial lithostratigraphic Unit B of cores SED-12 and SED-13 near the Alexander Channel [Lucchi et al., 2002]. Down core variations in NRM intensity and directions are not associated with changes in ARM and κ . High values of the grain size-dependent parameter ratio ARM/κ are observed in the

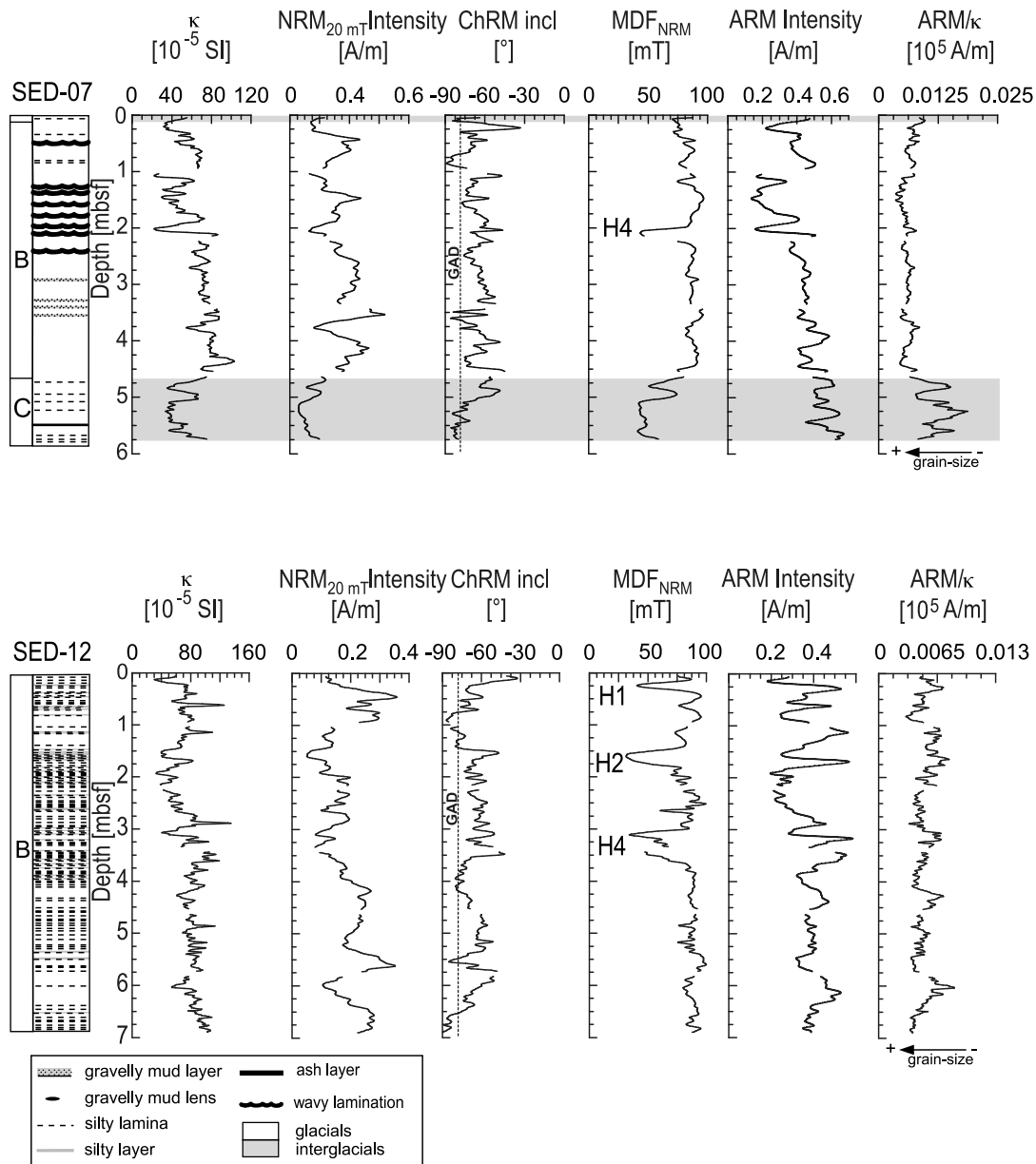


Figure 3a. Lithology and main magnetic parameters for cores SED-07 and SED-12. Low-field volume specific magnetic susceptibility (κ), $\text{NRM}_{20\text{mT}}$ intensity, ChRM inclination, MDF of the NRM, ARM intensity, and the grain size–dependent parameter ratio ARM/κ . The expected inclination for a geocentric axial dipole (GAD) field at the site latitude is also shown. The grey shaded area in the data for core SED-07 indicates interglacial lithostratigraphic units, and the thick black lines in the geological log for core SED-07 indicate volcanic ash layers/lenses after *Hillenbrand et al.* [2008b] and *Lucchi et al.* [2002]. H1, H2 and H4 indicate the intervals with MDF_{NRM} minima that are correlated to the North Atlantic Heinrich layers between 14 and 36 kyr BP [e.g., *Stoner et al.*, 1998; *Chapman et al.*, 2000; *Sagnotti et al.*, 2001].

interglacial layers (Figure 3a), which indicate fining grain size.

[25] Continuous monitoring of κ -T changes indicates Curie temperatures between 586 and 605°C (average = 597°C), which indicates the ubiquitous presence of Fe spinels with a composition similar to magnetite (Figure 4). A few samples (e.g., Figure 4h) have κ remaining between 640 and 680°C which indicates the presence of hematite.

The cooling curves often have higher κ than the heating curve, which indicates production of new magnetic phases during the continuous heating cycle. For some samples, the continuously monitored κ -T data show a slight decrease in susceptibility at 280–300°C, a feature also observed by *Sagnotti et al.* [2001], which they attributed to the presence of fine-grained monoclinic pyrrhotite. For such samples, we repeated the thermomagnetic experiment (Figure 4d) on a

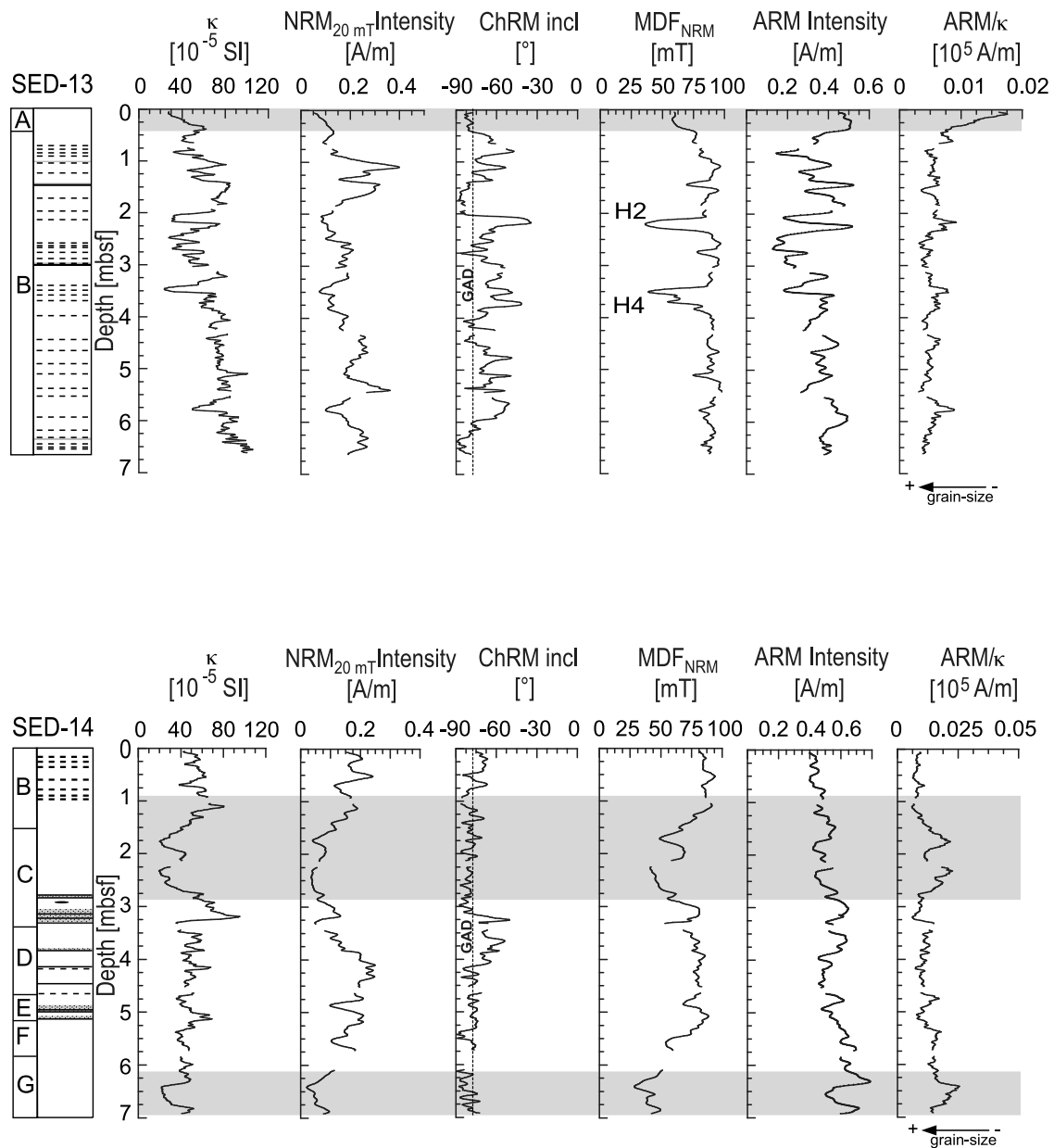


Figure 3b. Lithology and main magnetic parameters for cores SED-13 and SED-14. Parameters for core SED-14 were taken from *Macrì et al.* [2006], except for new data from the working halves of the core (see section 3.1). Low-field volume specific magnetic susceptibility (κ), $\text{NRM}_{20\text{mT}}$ intensity, ChRM inclination, MDF of the NRM, ARM intensity, and the grain size–dependent parameter ratio ARM/κ . The expected inclination for a GAD field at the site latitude is shown. The grey shaded areas indicate interglacial lithostratigraphic units and the thick black line in the geological log for core SED-14 indicate volcanic ash layers/lenses after *Hillenbrand et al.* [2008b] and *Lucchi et al.* [2002]. H2 and H4 indicate the intervals with MDF_{NRM} minima that are correlated to the North Atlantic Heinrich layers between 14 and 36 kyr BP [e.g., *Stoner et al.*, 1998; *Chapman et al.*, 2000; *Sagnotti et al.*, 2001].

new sample from the same level. The κ -T runs were first stopped at 350°C (red line in Figure 4d) to detect the pyrrhotite Curie temperature [Dekkers, 1989] which should be evident during both heating and cooling cycles [Hornig and Roberts, 2006]. The heating-cooling cycle was then repeated from room temperature up to 700°C (black line in

Figure 4d). The major decrease observed above 300°C is not reversible during the cooling cycle, and it is not present during the second heating run. If monoclinic pyrrhotite were stable to heating, this experiment should give an indication of a Curie temperature at 325°C [Dekkers, 1989] during both heating and cooling cycles [e.g., *Hornig and Roberts*, 2006,

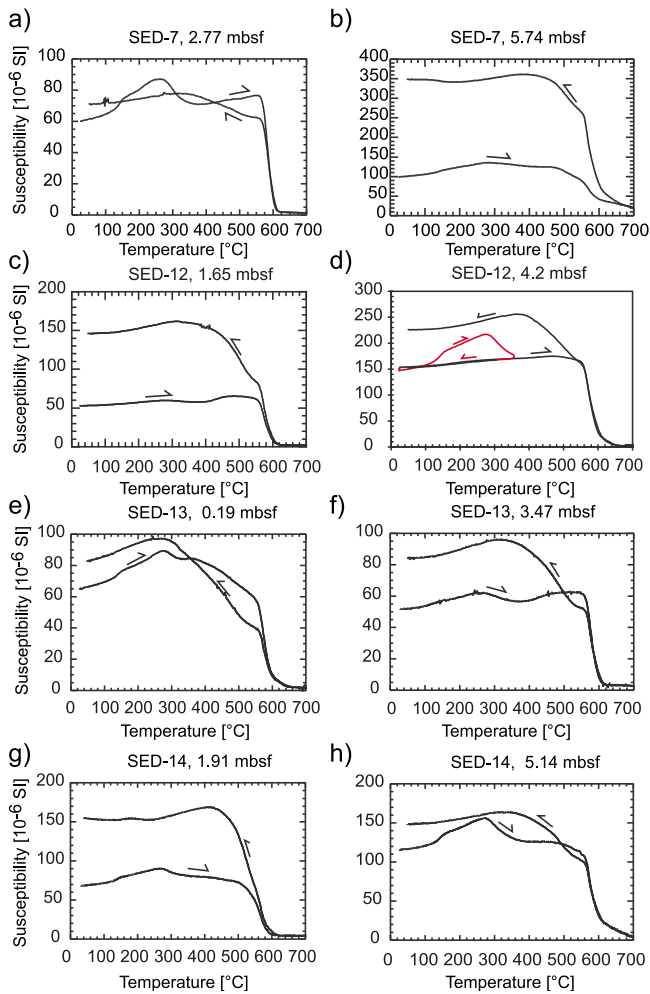


Figure 4. (a–h) Temperature dependence of low-field magnetic susceptibility (up to 700°C) for representative samples from drift 7. Curie temperatures for heating curves are 605°C (Figure 4a), 590°C (Figure 4b), 599°C (Figure 4c), 602°C (Figure 4d), 594°C (Figure 4e), 603°C (Figure 4f), 586°C (Figure 4g), and 600°C (Figure 4h) (average = 597°C). Figure 4d shows heating-cooling cycle up to 350°C (red line) followed by a standard cycle up to 700°C (black line). See text for discussion.

Figures 4c and 4d]. The peak in the κ -T runs (Figure 4) and the low temperature (<400°C) thermal instability in both κ -T runs may be caused by the presence of greigite (Fe_3S_4) [e.g., Roberts, 1995; Roberts *et al.*, 1999, 2011].

[26] Hysteresis ratios for samples from drift 7 are characterized by M_{rs}/M_s values between 0.08 and 0.32 and B_{cr}/B_c ratios between 2.72 and 10.99 that plot, mostly, in the PSD grain size range for pure magnetite ($0.5 < d < 10 \mu\text{m}$) [Day *et al.*, 1977] (Figure 5). However, the hysteresis data do not fall on the SD multidomain (MD) mixing line for magnetite, but have higher B_{cr}/B_c values, which might result from a contribution from SP particles [Dunlop, 2002].

[27] FORC distributions on representative intervals (Figure 5) indicate complex mixtures of grains (in terms of grain size and coercivities) with the dominance of SD particles with low magnetostatic interactions (e.g., SED-14, 1.89 mbsf) [cf. Roberts *et al.*, 2000] and, again, variable proportions of SP particles, which are sometimes evident from the secondary peak at the origin of the FORC diagram (e.g., SED-14, 3.8 mbsf; SED-12, 4.4 mbsf; SED-13, 0.19 mbsf) [Pike *et al.*, 2001]. Coarse grains in the MD range have low coercivities and FORC distributions that diverge toward the B_u axis (e.g., SED-13, 2.24 mbsf; SED-13, 1.08 mbsf) [cf. Roberts *et al.*, 2000].

[28] IRM acquisition curves for sediment chips indicate that saturation is nearly reached at fields of about 0.5 T for all samples (Figure 6), but they continue to increase above 0.3 T where magnetite should be fully saturated. This suggests the dominance of a low to moderate coercivity mineral with the presence of a higher coercivity mineral.

[29] Macri *et al.* [2006] showed that in drift 7 sediments the median destructive field of the NRM (MDF_{NRM} , i.e., the peak AF applied to reduce the initial NRM intensity by 50%) is related to B_{cr} . The MDF_{NRM} is generally higher (75 to 90 mT) in the glacial lithostratigraphic units and lower (30 to 60 mT) in both the interglacial units and in some thin (a few tens of centimeters thick) intervals within glacial unit B (Figure 3a). These thin, low- MDF_{NRM} intervals have also been observed at sites SED-02 and SED-04 by Sagnotti *et al.* [2001] who correlated them to Heinrich events 1 to 6 in the North Atlantic. Sagnotti *et al.* [2001] argued that this magnetic response reflects a dominance of detrital magnetite (for $\text{MDF}_{\text{NRM}} < 60$ mT) and pyrrhotite (for $\text{MDF}_{\text{NRM}} > 60$ mT), respectively. According to Macri *et al.* [2006], this dual magnetic behavior corresponds to values of $B_{cr} < \sim 65$ –70 mT and $B_{cr} > \sim 70$ mT, respectively.

4.2.2. Magnetic Mineralogy of Sediments From Drifts 4 and 5

[30] As for drift 7 samples, dual mineral magnetic behavior is apparent on drifts 5 and 4, where larger B_{cr} values are also associated with large $\text{SIRM}/\chi_{\text{lf}}$ values (Figure 7). However, here the response is not related to the lithostratigraphic units, but to the geographical location of the cores, with some Unit B sediments dominated by high coercivity behavior ($B_{cr} = 60$ –85 mT, e.g., core PC108) and

Figure 5. Plot of M_r/M_s versus B_{cr}/B_c [Day *et al.*, 1977] for representative samples from sediment cores recovered from drift 7, with hysteresis parameters and FORC distributions indicated for selected samples. Numbers along the curves on the Day plot are volume fractions of the soft component (SP or MD) in mixtures with SD grains [after Dunlop, 2002]. Curves with SP-SD mixtures have grain sizes indicated for the SP fraction. The FORC distributions for these samples indicate complex mixtures of grains with a dominance of SD particles with low magnetostatic interactions (e.g., SED-14, 1.89 mbsf) [cf. Roberts *et al.*, 2000] and variable proportions of SP particles, which are sometimes evident from the secondary peak at the origin of the FORC diagram (e.g., SED-14, 3.8 mbsf; SED-12, 4.4 mbsf; SED-13, 0.19 mbsf) [Pike *et al.*, 2001]. Coarse grains in the MD range have low coercivities and FORC distributions that diverge toward the B_u axis (e.g., SED-13, 2.24 mbsf; SED-13, 1.08 mbsf).

others dominated by lower coercivity behavior ($B_{cr} = 35\text{--}50\text{ mT}$) (Figure 7). Interglacial lithostratigraphic units A and C possess high and intermediate B_{cr} values. When compared with data from synthetic and sized magnetic oxides [Peters and Dekkers, 2003], B_{cr} and SIRM/ χ_{lf} data for cores

from drifts 4 and 5 suggest behavior that is incompatible with magnetic iron sulfides, but that is compatible with magnetite (Figure 7). Moreover, our samples have a larger range of B_{cr} values that do not overlap those for the laboratory-prepared materials.

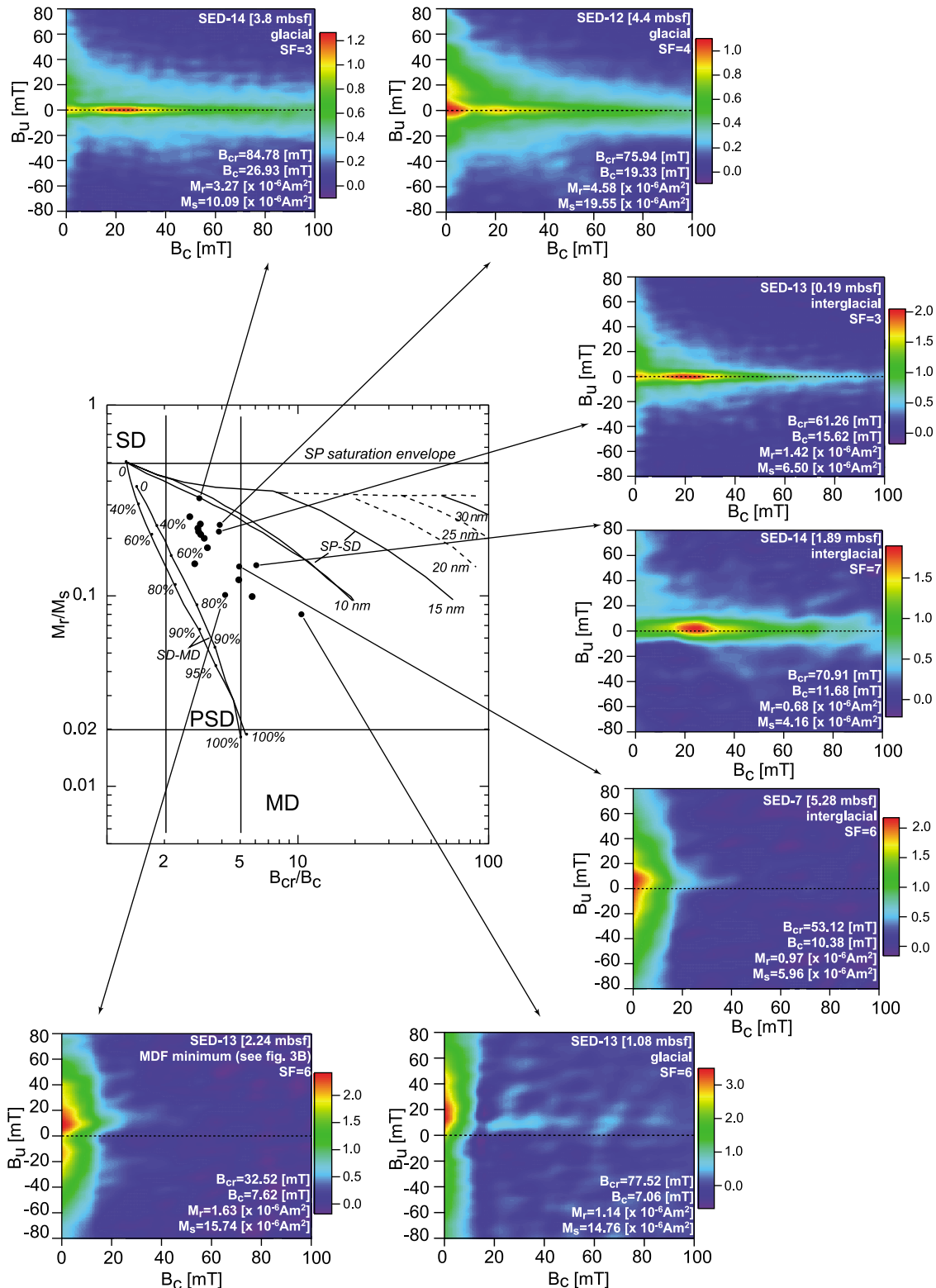


Figure 5

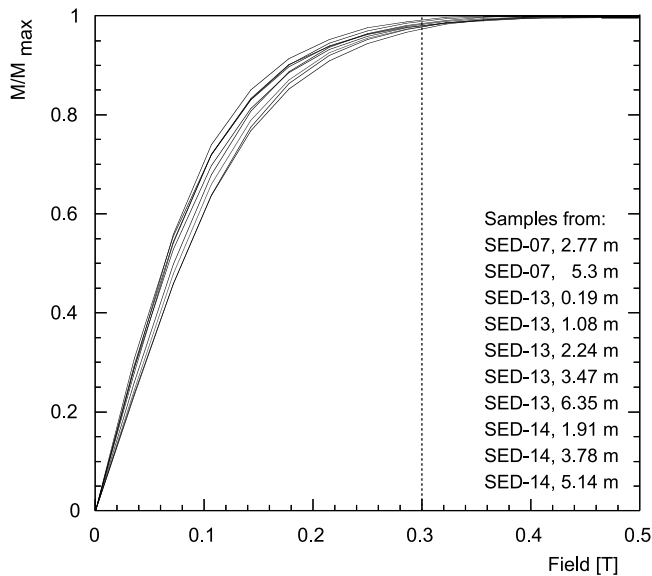


Figure 6. IRM acquisition curves for representative samples from cores SED-07, SED-13, and SED-14.

[31] Thermal demagnetization of orthogonal IRM results indicate the importance of the magnetite Curie temperature at around 600°C. Heating produces both low (<400°C) and high (>500°C) temperature mineralogical alteration as suggested by susceptibility measurements at each thermal demagnetization step (Figures 8a–8d). Low-temperature IRM data consistently indicate the magnetite Verwey transition at ~111 K (Figures 8e and 8f). X-ray diffraction results for magnetic mineral extracts also indicate that magnetite is dominant, with lattice constants of 8.388 to 8.405 Å (Figure 9). These values combined with the Curie temperatures, indicate that the titanomagnetites are slightly oxidized ($z < 0.3$), with low-ulvöspinel contents ($x < 0.1$) according to results from the synthetic samples of *Nishitani and Kono* [1983]. One of the magnetic extracts (from a depth of 356 cm in core PC108; Figure 9) possibly contains small amounts of hematite. Mean percentages of frequency-dependent magnetic susceptibility ($\% \chi_{fd}$) are 1.8% ($\sigma = 0.7$, $n = 303$), with an average percentage of IRM acquired between 0.3 and 1 Tesla of 1.2% ($\sigma = 0.6$, $n = 303$), which indicates that SP magnetite and hematite contributions are low.

[32] No pyrrhotite is apparent in the X-ray diffraction results for the magnetic extracts (Figure 9), and the low-temperature magnetic transition for pyrrhotite near 34 K [Dekkers, 1989; Rochette et al., 1990] is not present in the IRM unblocking data (Figures 8e and 8f). Unblocking up to ~300°C observed in the thermal demagnetization of orthogonal IRM data (Figure 8) is common in greigite dominated magnetizations, but is not restricted to greigite [Roberts et al., 2011]. No greigite is detected in the magnetic extracts (Figure 9), which implies that it is either absent or present only in low concentrations (the detection limit for the X-ray diffractometer used is between about 1 and 5%). Greigite therefore cannot account for the large drop (from ~20 to 300°C) in IRM intensity, in all coercivity fractions in the thermal demagnetization data (Figure 8).

Likewise, if greigite is present, it would be expected that the unblocking below 300°C would be dominantly in the medium and low coercivity fractions [Roberts et al., 2011].

[33] The mean sortable silt particle size (only measured in PC107) varies little (typically 16–22 microns) between samples or between lithostratigraphic units A to C. The magnetic parameters with the largest Pearson correlation coefficients with sortable silt size are $\chi/SIRM$ ($r = +0.50$) and $\chi_{ARM}/SIRM$ ($r = +0.36$), which suggests that 13–25% of the variability in these grain size specific magnetic parameters can be explained by changes in physical grain size.

4.3. Microscopy

[34] Characterization of opaque minerals in drift 7 samples, based on incident light polarized microscopy, complemented by EDS analysis of selected grains, indicate that detrital Fe oxides (interpreted as mostly titanomagnetite with low Ti substitutions), and Fe-Ti oxides (often Mn rich) are abundant. Moreover, occasional hexagonal Fe oxide grains (inferred to be hematite) were observed in a sample from the SED-12 core (from 4.40 mbsf). SEM and FESEM analysis revealed the occurrence of rare (<1%) Fe sulfides with irregular shapes dispersed within a clayey matrix in samples from glacial lithostratigraphic units of cores SED-07 and SED-12 (from 2.77 to 2.78 mbsf and 4.40 mbsf, respectively) and from both interglacial and glacial units of core SED-14 (from 1.89 and 3.80 mbsf). Fe sulfides occur as <1 μm aggregates in the glacial unit of core SED-07. These features are typical of authigenic Fe sulfide phases that grow during diagenesis [Rowan and Roberts, 2005, 2006]. The size of the aggregates is smaller than the interaction volume of the FESEM electron beam (1 μm), so that other elemental peaks (e.g., Si, Al, Mg) are recorded in addition to Fe and S peaks, which indicates contamination (or scattering of X-rays) with adjacent matrix minerals (e.g., quartz, chlorite). It has therefore not been possible to determine the chemistry of the sulfides.

[35] Optical microscopy of the magnetic extracts from drifts 4 and 5 indicates that ~40% of the volume is composed of angular detrital opaque phases up to about 20 μm in size. The remainder is mostly composed of quartz and feldspar, and smaller amounts of chlorite, diatom fragments and trace amounts of Cr spinels. The silicate particles often contain opaque inclusions. Under reflected light, a search was made for iron sulfides (having brassy-colored reflections) in the extracts, but neither nodules, framboids nor polyframboidal aggregates were found, which indicates the absence of magnetic sulfides greater than ~2 μm in size.

[36] These investigations indicate that low-Ti, partially oxidized titanomagnetite dominates the magnetic properties of all drift sediments. Magnetic iron sulfides make no significant contribution to the magnetic properties. The rare <1 μm sulfides detected by EDAX in the drift 7 sediments are probably derived from rock particles. Hematite probably makes a small contribution to the magnetic properties, but cannot account for the larger than normal B_{cr} values observed in most drift cores.

4.4. Age Models

[37] The magnetic susceptibility record from core SED-12 was correlated with the susceptibility record from core SED-02, which has been dated based on its RPI curve [Sagnotti

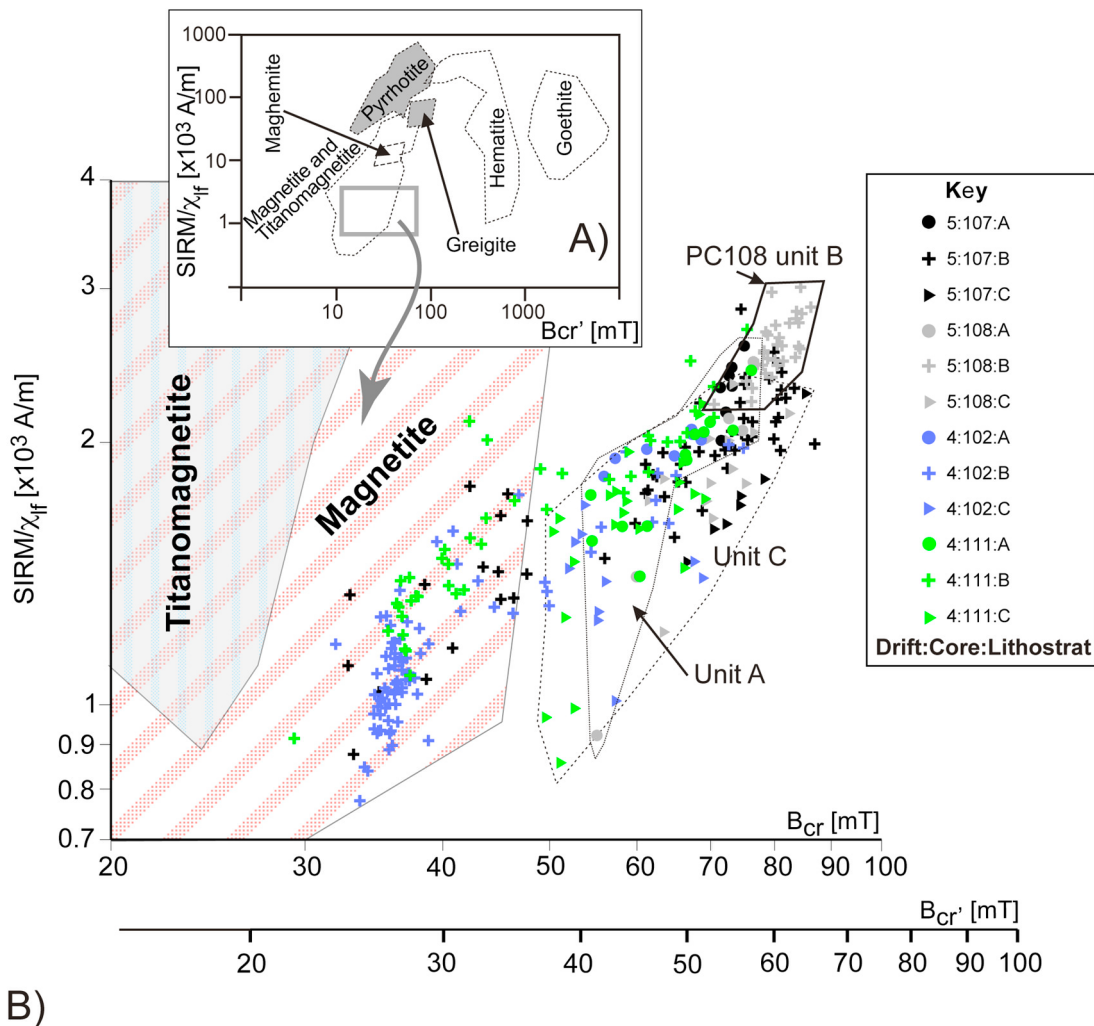


Figure 7. B_{cr} and $SIRM/\chi_{if}$ values for samples from drifts 4 and 5. Symbols correspond to different lithostratigraphic units and different colors correspond to different core numbers. Samples from lithostratigraphic units A and C fall in overlapping fields indicated by the outlined area. Parts of the fields for synthetic magnetite and titanomagnetite are indicated by inclined and vertical hash patterns, respectively, based on data from *Peters and Dekkers* [2003]. Their data are based on remanent acquisition coercivity (B_{cr}), rather than DC demagnetization remanent coercivity (B_{cr}), which has been calculated using a B_{cr}/B_{cr} ratio of 0.75 [*Peters and Dekkers*, 2003]. The full ranges of the data fields for magnetite, titanomagnetite, hematite, goethite, and iron sulfides are shown in the inset [from *Peters and Dekkers*, 2003].

et al., 2001]. After this matching (Figure 10a), the two susceptibility records are significantly correlated (Pearson correlation coefficient $r^2 = 0.80$), and the resulting age model indicates an age of 77 ka for the sediments at the base of core SED-12. Correlation of the magnetic susceptibility record from core SED-07 with those of RPI-dated cores SED-04 and SED-06 indicates an age of 122 ka for the oldest sediments at site SED-07 (Figure 10b). Our age model for core SED-07 is consistent with age constraints provided by tephra layers in Unit C [*Hillenbrand et al.*, 2008b]. Correlation of ARM/κ ratios for cores SED-12 and SED-13 indicates that core SED-13 spans the last 76 kyr (Figure 10c). Our age models for the drift 7 cores imply that average sedimentation rates are highest near the Alexander

Channel (12 cm/kyr in core SED-12 and 9 cm/kyr in core SED-13, respectively), where sedimentation is directly influenced by both turbidity and contour currents, relative to the rates recorded toward the crest of drift 7 (5 cm/kyr in core SED-07) [see also *Macri et al.*, 2006, Figure 6].

5. Discussion

[38] Previous investigations have demonstrated the potential of sedimentary sequences recovered from giant deep-sea drifts on the Pacific continental rise of the Antarctic Peninsula for reconstructing the late Neogene and Pleistocene paleoenvironmental history of West Antarctica [e.g., *Pudsey and Camerlenghi*, 1998; *Pudsey*, 2000; *Lucchi*

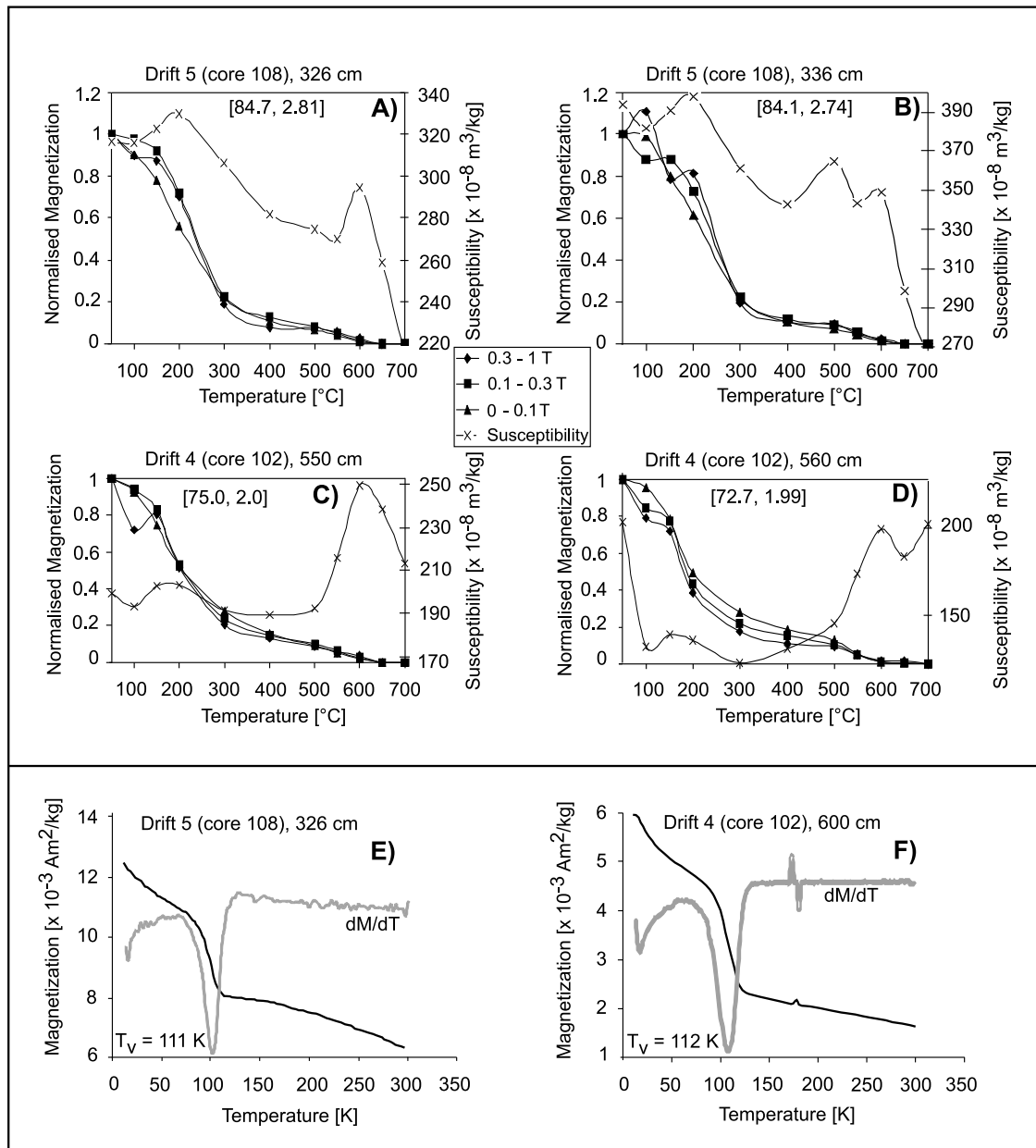


Figure 8. (a–d) Thermal demagnetization of a three-component IRM using orthogonal magnetic fields of 1 T, 0.3 T, and 0.1 T for samples from sediment cores recovered from drifts 4 and 5. In each case, the magnetically hard titanomagnetite fraction is important, and B_{cr} (in mT) and $SIRM_{1T}/\chi_{lf}$ (in $\times 10^3$ A/m) values are indicated in [], respectively. (e and f) Low-temperature demagnetization of an IRM acquired at 10 K for two of the samples shown above, with a clear transition temperature (T_V), which is interpreted as the Verwey transition. Plots of the magnetization derivatives dM/dT are indicated in gray.

et al., 2002; Hillenbrand and Ehrmann, 2005]. Detailed reconstructions of the sedimentary evolution of the drifts and their relationship to climate change and glacial history of the Antarctic Peninsula can only be carried out if a high-resolution and robust chronostratigraphic framework can be established for these drifts. Calcareous (micro)fossils are either absent or are not continuously present in the terrigenous, glaciomarine sediments from the Antarctic continental margin, which prevents application of reliable AMS ^{14}C dating or oxygen isotope stratigraphy. Age models with the

potential to resolve millennial climate variations can be established for these sequences by measuring their RPI records and correlating the RPI records to well-dated reference curves [Guyodo and Valet, 1999; Guyodo *et al.*, 2001; Sagnotti *et al.*, 2001; Stoner *et al.*, 2002; Macri *et al.*, 2006]. This dating technique, however, can only be successfully applied if it is convincingly demonstrated that the magnetic mineralogy of the drift sediments is suitable for reliable recording of the geomagnetic field. Our new microscopic observations and measurements on sediments and magnetic

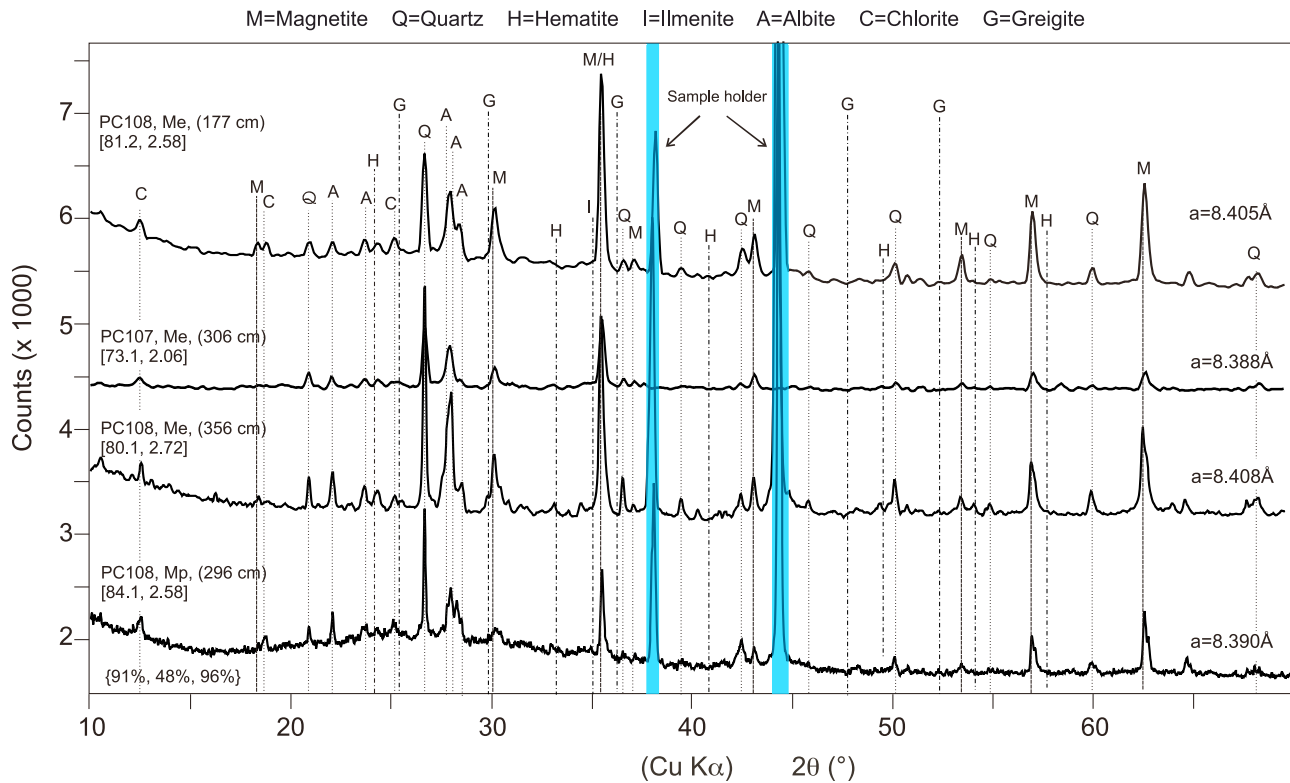


Figure 9. X-ray diffraction data for magnetic extracts of samples from drift 5 (cores PC108 and PC107). In each case, the diffraction profiles represent samples in which the ‘hard titanomagnetite’ fraction is important. The upper three extracts were produced using a quick extraction method, flagged as the M_e method [Hounslow and Maher, 1999] to limit oxidation of potential iron sulfides in the samples. For the lowest trace from the sample at a depth of 296 cm in core PC108 the magnetic probe (M_p) method was applied [Hounslow and Maher, 1999]. Magnetic mineral extraction efficiencies of χ_{If} , ARM and $SIRM_{IT}$ are shown in { }; a = magnetic lattice constant. B_{cr} (in mT) and $SIRM_{IT}/\chi_{If}$ (in $\times 10^3$ A/m) values are indicated in [], respectively.

extracts, taken from late Pleistocene sediment cores recovered from the drifts on the western Antarctic Peninsula rise, demonstrate that these studied sequences have a complex magnetic mineralogy. Our results indicate that detrital PSD titanomagnetite ($z < 0.3$; $x < 0.1$) represents the main magnetic mineral in the drift sediments. Based on thermomagnetic, low temperature, X-ray diffraction and microscopy data, we find no evidence for either pyrrhotite or greigite, which contrasts with the inferences of Sagnotti *et al.* [2001]. Rare Fe sulfides are present, but they appear to be restricted to inclusions within clastic particles. Hematite appears to be present in minor amounts. Instead, we consider the presence of “magnetically hard titanomagnetite” as the most likely explanation of the observed higher coercivities, which are in excess of those known from synthetic titanomagnetites [Peters and Dekkers, 2003]. Similarly, single-domain bacterial magnetite arranged in chains has remanent coercivities of up to 45–50 mT [Pan *et al.*, 2005], which are lower than those found in some of our sediments. The remanent coercivities in excess of 60 mT are similar to those reported from silicate-hosted titanomagnetites [Feinberg *et al.*, 2005]. Particle elongation and internal subdivision (resulting in magnetostatically noninteracting single-domain particles) are key factors that produce the high remanent coercivities.

Unlike the data of Brachfeld *et al.* [2001] from ODP Site 1096 near the crest of drift 7 [Barker *et al.*, 1999a, 2002], we find no evidence for high defect concentrations or substantial cation substitution, which could account for such large B_{cr} values. In drift 7, the supply of magnetically hard titanomagnetite increased significantly during glacial periods, when the Antarctic Peninsula Ice Sheet reached its maximum extent across the adjacent shelf, which resulted in a higher terrigenous input to the continental rise [Pudsey, 2000; Lucchi *et al.*, 2002; Hillenbrand and Ehrmann, 2005]. The same appears not to be the case on drifts 4 and 5, where this hard magnetite component is not restricted to the glacial lithostratigraphic units of the corresponding sediment cores. We attribute these differences in magnetic mineralogy between the drifts to regional differences in the provenance of the terrigenous detritus supplied to the continental rise. Regionally variable provenance has previously been inferred from the inorganic chemical composition of drift sediments along the margin [Pudsey, 2000], their clay mineral composition [Hillenbrand and Ehrmann, 2002; Lucchi *et al.*, 2002], their magnetic susceptibility values [Pudsey, 2000] and from the petrological composition of their coarse-grained fractions [Cowan *et al.*, 2008].

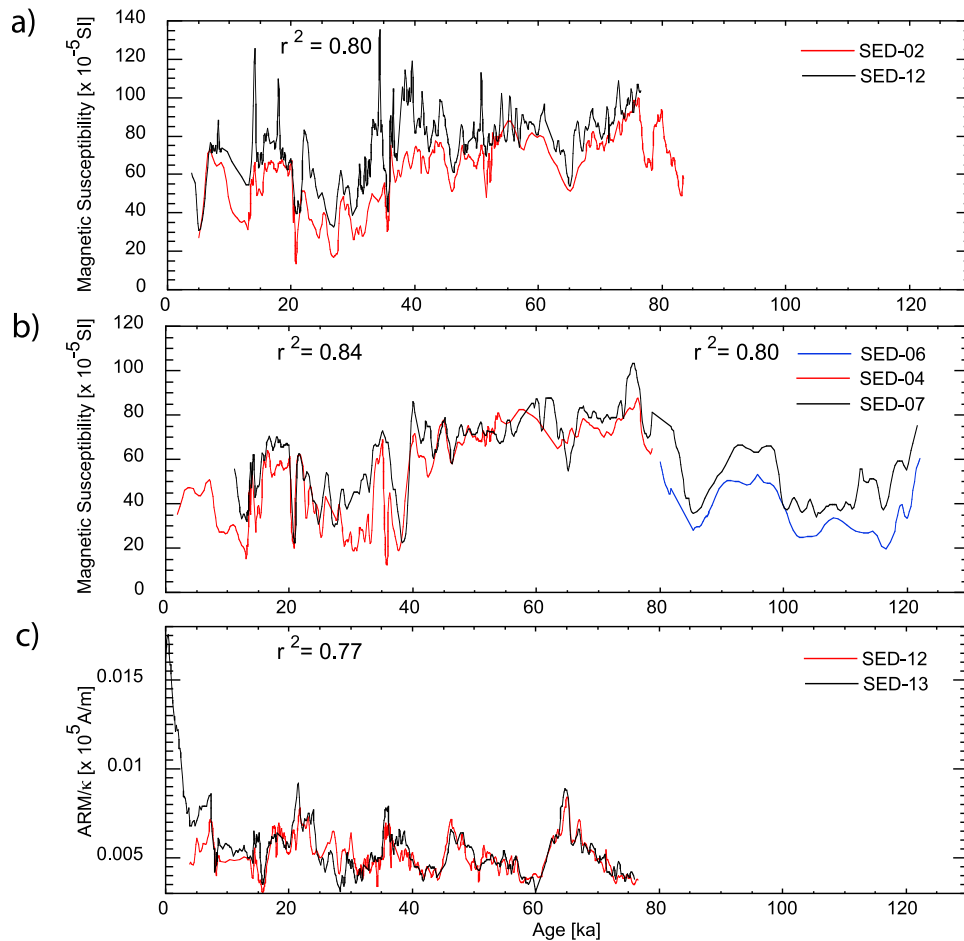


Figure 10. Establishment of age models for the studied cores from drift 7 by correlation of the magnetic susceptibility profiles of cores (a) SED-12 and (b) SED-7, and of the ARM/ κ profile for core (c) SED-13 with the corresponding parameters from RPI-dated cores from drift 7.

[39] We have developed new high-resolution age models by analyzing magnetic properties of three sediment cores recovered near the Alexander Channel and near the crest of drift 7, respectively. High-resolution magnetic measurements on u channel samples facilitated correlation of these cores with RPI-dated cores from the same drift. The resulting age models document a relatively long history of sedimentation in core SED-07, which has an age of 122 ka at its base. Conversely, the sedimentation rates are much higher near Alexander Channel (cores SED-12 and SED-13), where sedimentation is directly influenced by turbidity currents and bottom currents. Consequently, the oldest sediments recovered at these sites are younger than 80 ka.

[40] Similar to cores from drift 7 studied by *Sagnotti et al.* [2001], the MDF_{NRM} curves in cores SED-07, SED-12 and SED-13 reveal distinct minima within intervals of glacial lithostratigraphic Unit B (Figure 2d) that correlate to Heinrich events 1 to 4 in the northern hemisphere (Figures 3a and 3b). *Sagnotti et al.* [2001] argued that, in contrast to the other glacial sediments of Unit B, diagenetic pyrrhotite formation was drastically or completely suppressed in these layers due to a major reduction in organic matter supply to the seafloor, which resulted from significantly decreased biological productivity, caused by intensification of sea ice

coverage in response to cooling. This explanation conflicts with observations that Heinrich events seem to coincide with (1) periods of atmospheric warming in Antarctica [e.g., *EPICA Community Members*, 2006] and (2) enhanced plankton productivity in the Southern Ocean, both to the north [*Sachs and Anderson*, 2005] and south [*Anderson et al.*, 2009] of the Antarctic Polar Front. Furthermore, monoclinic pyrrhotite grows slowly in sediments [*Horng and Roberts*, 2006], so diagenetic pyrrhotite growth is unlikely to give rise to reliable recording of RPI signals. Our more comprehensive magnetic mineralogical data indicate an absence of pyrrhotite in drift sediments from the Antarctic Peninsula margin, which is inconsistent with the interpretation of *Sagnotti et al.* [2001]. Moreover, our magnetic mineralogical findings indicate negligible to trace amounts of iron sulfides in the glacial drift sediments and thus do not confirm the suggestion of *Lucchi and Rebesco* [2007] that oxygen-depleted deep and bottom waters bathed the Antarctic Peninsula continental rise during late Pleistocene glacial periods.

[41] Our data suggest that the MDF_{NRM} minima recorded in the drift 7 sediments, which have been associated with Heinrich events, are related to changes in the delivery of Fe oxides with differing microstructural characteristics. These

short-term temporal shifts in sediment provenance were probably caused by the warming events that modified the delivery of glaciogenic detritus to the drifts by affecting either the bottom current transport of fine-grained detritus along the continental rise or the glacial drainage pattern on the shelf and in the hinterland.

6. Conclusions

[42] We present new paleomagnetic and robust mineral magnetic data from drifts located along the Pacific continental margin of the Antarctic Peninsula which evaluate the chronology and mineral magnetic integrity of these sediments.

[43] Our chronology document a relatively long history of sedimentation in core SED-07, recovered near the drift crest, which has an age of 122 ka at its base. Sedimentation rates are relatively high at sites located close to the Alexander Channel system where sedimentation is directly influenced by both turbidity and contour currents.

[44] Low- and high-temperature magnetic measurements in conjunction with microscopic and mineralogic observations indicate that PSD detrital titanomagnetite is the dominant magnetic mineral in these drift sediments, which occurs as both a low-coercivity form (similar to laboratory-synthesized titanomagnetite), and a high-coercivity form. These two forms vary in amount and stratigraphic distribution across the drifts. This robust and comprehensive mineral magnetic data indicate an absence of pyrrhotite or greigite in drift sediments from the Antarctic Peninsula margin, contradictory to the interpretation of Sagnotti *et al.* [2001].

[45] The observed change of magnetic mineralogy in sediments deposited during Heinrich events on drift 7 (four intervals that are correlated to the North Atlantic Heinrich layers between 14 and 36 kyr BP) appears to be related to warming periods, which temporarily modified the normal glacial transport pathways of glaciogenic detritus to and along the continental rise and thus resulted in deposition of sediments with a different provenance.

[46] **Acknowledgments.** This work was supported by Italian PNRA grants for the SEDANO-I and -II projects and by the BAS Palaeo-Ice Sheets and SAGES-500K projects. Reviews by Andrew P. Roberts, Stefanie Brachfeld, an anonymous reviewer, and the Associate Editor helped to improve the manuscript. We are grateful to Carol Pudsey, Ian Hawkes, and Barbara Maher, who all assisted in a variety of ways and to the captains, officers, crew, and scientists who participated in the various cruises.

References

- Acton, G. D., M. Okada, B. M. Clement, S. P. Lund, and T. Williams (2002), Paleomagnetic overprints in ocean sediment cores and their relationship to shear deformation caused by piston coring, *J. Geophys. Res.*, *107*(B4), 2067, doi:10.1029/2001JB000518.
- Ambias, D., R. Urgeles, M. Canals, A. M. Calafat, M. Rebesco, A. Camerlenghi, F. Estrada, M. De Batist, and J. E. Hughes-Clarke (2006), Relationship between continental rise development and palaeo-ice sheet dynamics, Northern Antarctic Peninsula Pacific margin, *Quat. Sci. Rev.*, *25*, 933–944, doi:10.1016/j.quascirev.2005.07.012.
- Anderson, R. F., S. Ali, L. I. Bradtmiller, S. H. H. Nielsen, M. Q. Fleisher, B. E. Anderson, and L. H. Burckle (2009), Wind-driven upwelling in the Southern Ocean and the deglacial rise in atmospheric CO₂, *Science*, *323*, 1443–1448, doi:10.1126/science.1167441.
- Barker, P. F., et al. (1999a), *Proceedings of the Ocean Drilling Program Initial Reports*, vol. 178, Ocean Drill. Program, College Station, Tex., doi:10.2973/odp.proc.ir.178.1999.
- Barker, P. F., P. J. Barrett, A. K. Cooper, and P. Huybrechts (1999b), Antarctic glacial history from numerical models and continental margin sediments, *Palaeogeogr. Palaeoclimatol. Palaeoecol.*, *150*, 247–267, doi:10.1016/S0031-0182(98)00224-7.
- Barker, P. F., A. Camerlenghi, G. D. Acton, and A. T. S. Ramsay (Eds.) (2002), *Proceedings of the Ocean Drilling Program Scientific Results*, vol. 178, Ocean Drill. Program, College Station, Tex., doi:10.2973/odp.proc.sr.178.2002.
- Barker, P. F., G. M. Filippelli, F. Florindo, E. E. Martin, and H. D. Scher (2007), Onset and role of the Antarctic Circumpolar Current, *Deep Sea Res., Part II*, *54*, 2388–2398, doi:10.1016/j.dsr2.2007.07.028.
- Brachfeld, S. A., Y. Guyodo, and G. D. Acton (2001), Data report: The magnetic mineral assemblage of hemipelagic drifts, ODP Site 1096, *Proc. Ocean Drill. Program Sci. Results*, *178*, 1–10, doi:10.2973/odp.proc.sr.178.233.2001.
- Camerlenghi, A., A. Crise, C. J. Pudsey, E. Accerboni, R. Laterza, and M. Rebesco (1997a), Ten-month observation of the bottom current regime across a sediment drift of the Pacific margin of the Antarctic Peninsula, *Antarct. Sci.*, *9*, 426–433, doi:10.1017/S0954102097000552.
- Camerlenghi, A., M. Rebesco, and C. J. Pudsey (1997b), High resolution terrigenous sedimentary record of a sediment drift on the Antarctic Peninsula Pacific margin (Initial Results of the 'SEDANO' Program), in *The Antarctic Region: Geological Evolution and Processes*, edited by C. A. Ricci, pp. 705–710, Terra Antarctica, Siena, Italy.
- Carter, L., I. N. McCave, and M. J. M. Williams (2008), Circulation and water masses of the Southern Ocean: A review, in *Antarctic Climate Evolution*, *Dev. Earth Environ. Sci.*, vol. 8, pp. 85–114, edited by F. Florindo and M. Siebert, Elsevier, New York.
- Chapman, M. R., N. J. Shackleton, and J.-C. Duplessy (2000), Sea surface temperature variability during the last glacial-interglacial cycle: Assessing the magnitude and pattern of climate change in the North Atlantic, *Palaeogeogr. Palaeoclimatol. Palaeoecol.*, *157*, 1–25, doi:10.1016/S0031-0182(99)00168-6.
- Cowan, E. A., C.-D. Hillenbrand, L. E. Hassler, and M. T. Ake (2008), Coarse-grained terrigenous sediment deposition on continental rise drifts: A record of Plio-Pleistocene glaciation on the Antarctic Peninsula, *Palaeogeogr. Palaeoclimatol. Palaeoecol.*, *265*, 275–291, doi:10.1016/j.palaeo.2008.03.010.
- Day, R., M. Fuller, and V. A. Schmidt (1977), Hysteresis properties of titanomagnetites: Grain-size and compositional dependence, *Phys. Earth Planet. Inter.*, *13*, 260–267, doi:10.1016/0031-9201(77)90108-X.
- Dekkers, M. J. (1989), Magnetic properties of natural pyrrhotite. II. High- and low-temperature behaviour of J_{rs} and TRM as function of grain size, *Phys. Earth Planet. Inter.*, *57*, 266–283, doi:10.1016/0031-9201(89)90116-7.
- Dunlop, D. J. (2002), Theory and application of the Day plot (M_{rs}/M_s versus H_{cr}/H_c): 1. Theoretical curves and tests using titanomagnetite data, *J. Geophys. Res.*, *107*(B3), 2056, doi:10.1029/2001JB000486.
- EPICA Community Members (2006), One-to-one hemispheric coupling of glacial climate variability in Greenland and Antarctica, *Nature*, *444*, 195–198, doi:10.1038/nature05301.
- Feinberg, J. M., G. R. Scott, P. R. Renne, and H.-R. Wenk (2005), Exsolved magnetite inclusions in silicates: Features determining their remanence behavior, *Geology*, *33*, 513–516, doi:10.1130/G21290.1.
- Florindo, F., and L. Sagnotti (1995), Palaeomagnetism and rock magnetism in the upper Pliocene Valle Ricca (Rome, Italy) section, *Geophys. J. Int.*, *123*, 340–354, doi:10.1111/j.1365-246X.1995.tb06858.x.
- Florindo, F., and M. Siebert (Eds.) (2008), *Antarctic Climate Evolution*, *Dev. Earth Environ. Sci.*, vol. 8, pp. 1–593, Elsevier, New York.
- Florindo, F., G. S. Wilson, A. P. Roberts, L. Sagnotti, and K. L. Verosub (2005), Magnetostratigraphic chronology of a Late Eocene to early Miocene glaciomarine succession from the Victoria Land Basin, Ross Sea, Antarctica, *Global Planet. Change*, *45*, 207–236, doi:10.1016/j.gloplacha.2004.09.009.
- Florindo, F., D. B. Karner, F. Marra, P. R. Renne, A. P. Roberts, and R. Weaver (2007), Radioisotopic age constraints for Glacial Terminations IX and VII from aggradational sections of the Tiber River delta in Rome, Italy, *Earth Planet. Sci. Lett.*, *256*, 61–80, doi:10.1016/j.epsl.2007.01.014.
- Giorgetti, A., A. Crise, R. Laterza, L. Perini, M. Rebesco, and A. Camerlenghi (2003), Water masses and bottom boundary layer dynamics above a sediment drift of the Antarctic Peninsula Pacific Margin, *Antarct. Sci.*, *15*, 537–546, doi:10.1017/S0954102003001652.
- Guyodo, Y., and J.-P. Valet (1999), Global changes in intensity of the Earth's magnetic field during the past 800 kyr, *Nature*, *399*, 249–252, doi:10.1038/20420.
- Guyodo, Y., G. D. Acton, S. Brachfeld, and J. E. T. Channell (2001), A sedimentary paleomagnetic record of the Matuyama chron from the Western Antarctic margin (ODP Site 1101), *Earth Planet. Sci. Lett.*, *191*, 61–74, doi:10.1016/S0012-821X(01)00402-2.

- Harland, R., and C. J. Pudsey (1999), Dinoflagellate cysts from sediment traps deployed in the Bellingshausen, Weddell and Scotia seas, Antarctica, *Mar. Micropaleontol.*, **37**, 77–99, doi:10.1016/S0377-8398(99)00016-X.
- Harrison, R. J., and J. M. Feinberg (2008), FORCinel: An improved algorithm for calculating first-order reversal curve distributions using locally weighted regression smoothing, *Geochem. Geophys. Geosyst.*, **9**, Q05016, doi:10.1029/2008GC001987.
- Hawkes, I. J., M. W. Hounslow, C. J. Pudsey, and B. A. Maher (2003), Sediment dispersal pathways from the western Antarctic Peninsula during the last glacial period and the significance of temporal fluctuations in magnetic properties, *Geophys. Res. Abstr.*, **5**, 11,099.
- Heinrich, H. (1988), Origin and consequences of cycling ice rafting in the northeast Atlantic Ocean during the past 130,000 years, *Quat. Res.*, **29**, 142–152, doi:10.1016/0033-5894(88)90057-9.
- Hemming, S. R. (2004), Heinrich events: Massive late Pleistocene detritus layers of the North Atlantic and their global climate imprint, *Rev. Geophys.*, **42**, RG1005, doi:10.1029/2003RG000128.
- Hernández-Molina, F. J., R. D. Larter, A. Maldonado, and J. Rodríguez-Fernández (2006), Evolution of the Antarctic Peninsula Pacific margin offshore from Adelaide Island since the late Miocene: An example of a glacial passive margin, *Terra Antarct. Rep.*, **12**, 81–90.
- Hillenbrand, C.-D., and W. Ehrmann (2002), Distribution of clay minerals in drift sediments on the continental rise west of the Antarctic Peninsula, ODP Leg 178, Sites 1095 and 1096, *Proc. Ocean Drill. Program Sci. Results*, **178**, 1–29, doi:10.2973/odp.proc.sr.178.224.2001.
- Hillenbrand, C.-D., and W. Ehrmann (2005), Late Neogene to Quaternary environmental changes in the Antarctic Peninsula region: Evidence from drift sediments, *Global Planet. Change*, **45**, 165–191, doi:10.1016/j.gloplacha.2004.09.006.
- Hillenbrand, C.-D., A. Camerlenghi, E. A. Cowan, F. J. Hernández-Molina, R. G. Lucchi, M. Rebesco, and G. Uenzelmann-Neben (2008a), The present and past bottom-current flow regime around the sediment drifts on the continental rise west of Antarctic Peninsula, *Mar. Geol.*, **255**, 55–63, doi:10.1016/j.margeo.2008.07.004.
- Hillenbrand, C.-D., S. G. Moreton, A. Caburlotto, C. J. Pudsey, R. G. Lucchi, J. L. Smellie, S. Benetti, H. Grobe, J. B. Hunt, and R. D. Larter (2008b), Volcanic time-markers for Marine Isotopic Stages 6 and 5 in Southern Ocean sediments and Antarctic ice cores: Implications for tephra correlations between palaeoclimatic records, *Quat. Sci. Rev.*, **27**, 518–540, doi:10.1016/j.quascirev.2007.11.009.
- Horng, C.-S., and A. P. Roberts (2006), Authigenic or detrital origin of pyrrhotite in sediments?: Resolving a paleomagnetic conundrum, *Earth Planet. Sci. Lett.*, **241**, 750–762, doi:10.1016/j.epsl.2005.11.008.
- Hounslow, M. W., and B. A. Maher (1996), Quantitative extraction and analysis of carriers of magnetization in sediments, *Geophys. J. Int.*, **124**, 57–74, doi:10.1111/j.1365-246X.1996.tb06352.x.
- Hounslow, M. W., and B. A. Maher (1999), Laboratory procedures for quantitative extraction and analysis of magnetic minerals from sediments, in *Environmental Magnetism, A Practical Guide, Tech. Guide*, vol. 6, edited by J. Walden, F. Oldfield, and J. Smith, pp. 139–164, Quat. Res. Assoc., Lancaster, U. K.
- Hrouda, F. (1994), A technique for the measurements of thermal changes of magnetic susceptibility of weakly magnetic rocks by the CS-2 Apparatus and KLY-2 Kappabridge, *Geophys. J. Int.*, **118**, 604–612, doi:10.1111/j.1365-246X.1994.tb03987.x.
- Intergovernmental Panel on Climate Change (IPCC) (2007), Summary for policymakers, in *Climate Change 2007: The Physical Science Basis – Contribution of Working Group I to the Fourth Assessment Report of the Intergovernmental Panel on Climate Change*, edited by S. Solomon et al., 996 pp., Cambridge Univ. Press, New York.
- King, J. C., J. Turner, G. J. Marshall, W. M. Connolley, and T. A. Lachlan-Cope (2003), Antarctic Peninsula climate variability and its causes as revealed by analysis of instrumental records, in *Antarctic Peninsula Climate Variability: Historical and Palaeoenvironmental Perspectives*, *Antarct. Res. Ser.*, no. 79, edited by E. Domack et al., pp. 17–30, AGU, Washington, D. C.
- Kirschvink, J. L. (1980), The least-square line and plane and the analysis of palaeomagnetic data, *Geophys. J. R. Astron. Soc.*, **62**, 699–718.
- Lowrie, W. (1990), Identification of ferromagnetic minerals in a rock by coercivity and unblocking temperature profiles, *Geophys. Res. Lett.*, **17**, 159–162, doi:10.1029/GL017i002p00159.
- Lucchi, R. G., and M. Rebesco (2007), Glacial contourites on the Antarctic Peninsula margin: Insight for palaeoenvironmental and palaeoclimatic conditions, *Spec. Publ. Geol. Soc. London*, **276**, 111–127, doi:10.1144/GSL.SP.2007.276.01.06.
- Lucchi, R. G., M. Rebesco, A. Camerlenghi, M. Busetti, L. Tomadin, G. Villa, D. Persico, C. Morigi, M. C. Bonci, and G. Giorgetti (2002), Mid-late Pleistocene glacial marine sedimentary processes of a high-latitude, deep-sea sediment drift (Antarctic Peninsula Pacific margin), *Mar. Geol.*, **189**, 343–370, doi:10.1016/S0025-3227(02)00470-X.
- Macri, P., L. Sagnotti, R. G. Lucchi, and M. Rebesco (2006), A stacked record of relative geomagnetic paleointensity for the past 270 kyr from the western continental rise of the Antarctic Peninsula, *Earth Planet. Sci. Lett.*, **252**, 162–179, doi:10.1016/j.epsl.2006.09.037.
- Mazaud, A. (2005), User-friendly software for vector analysis of the magnetization of long sediment cores, *Geochem. Geophys. Geosyst.*, **6**, Q12006, doi:10.1029/2005GC001036.
- Nishitani, T., and M. Kono (1983), Curie temperatures and lattice constant of oxidized titanomagnetite, *Geophys. J. R. Astron. Soc.*, **74**, 585–600.
- Ó Cofaigh, C., J. A. Dowdeswell, and C. J. Pudsey (2001), Late Quaternary iceberg rafting along the Antarctic Peninsula continental rise and in the Weddell and Scotia Seas, *Quat. Res.*, **56**, 308–321, doi:10.1006/qres.2001.2267.
- Paillard, D., L. Labeyrie, and P. Yiou (1996), Macintosh program performs time-series analysis, *Eos Trans. AGU*, **77**(39), 379, doi:10.1029/96EO00259.
- Pan, Y., N. Petersen, A. F. Davila, L. Zhang, M. Winklhofer, Q. Liu, M. Hanzlik, and R. Zhu (2005), The detection of bacterial magnetite in recent sediments of Lake Chiemsee (southern Germany), *Earth Planet. Sci. Lett.*, **232**, 109–123, doi:10.1016/j.epsl.2005.01.006.
- Peters, C., and M. J. Dekkers (2003), Selected room temperature magnetic parameters as a function of mineralogy, concentration and grain size, *Phys. Chem. Earth*, **28**, 659–667.
- Pike, C. R., A. P. Roberts, and K. L. Verosub (2001), First-order reversal curve diagrams and thermal relaxation effects in magnetic particles, *Geophys. J. Int.*, **145**, 721–730, doi:10.1046/j.0956-540x.2001.01419.x.
- Pudsey, C. J. (2000), Sedimentation on the continental rise west of the Antarctic Peninsula over the last three glacial cycles, *Mar. Geol.*, **167**, 313–338, doi:10.1016/S0025-3227(00)00039-6.
- Pudsey, C. J., and A. Camerlenghi (1998), Glacial-interglacial deposition on a sediment drift on the Pacific margin of the Antarctic Peninsula, *Antarct. Sci.*, **10**, 286–308, doi:10.1017/S0954102098000376.
- Rebesco, M., R. D. Larter, A. Camerlenghi, and P. F. Barker (1996), Giant sediment drifts on the continental rise west of the Antarctic Peninsula, *Geo Mar. Lett.*, **16**, 65–75, doi:10.1007/BF02020600.
- Rebesco, M., R. D. Larter, P. F. Barker, A. Camerlenghi, and L. E. Vanneste (1997), The history of sedimentation on the continental rise west of the Antarctic Peninsula, in *Geology and Seismic Stratigraphy of the Antarctic Margin, Part 2*, *Antarct. Res. Ser.*, no. 71, edited by P. F. Barker and A. K. Cooper, pp. 29–49, AGU, Washington, D. C.
- Rebesco, M., A. Camerlenghi, and C. Zanolla (1998), Bathymetry and morphogenesis of the continental margin west of the Antarctic Peninsula, *Terra Antarct.*, **5**, 715–725.
- Rebesco, M., C. J. Pudsey, M. Canals, A. Camerlenghi, P. F. Barker, F. Estrada, and A. Giorgetti (2002), Sediment drifts and deep-sea channel systems, Antarctic Peninsula Pacific Margin, in *Deep-Water Contourite Systems: Modern Drifts and Ancient Series, Seismic and Sedimentary Characteristics*, edited by D. A. V. Stow et al., *Mem. Geol. Soc. London*, **22**, 353–371.
- Rebesco, M., A. Camerlenghi, V. Volpi, C. Neagu, D. Accettella, B. Lindberg, A. Cova, F. Zgur, and the MAGICO party (2007), Interaction of processes and importance of contourites: Insights from the detailed morphology of sediment drift 7, Antarctica, in *Economic and Palaeoceanographic Significance of Contourite Deposits*, edited by A. R. Viana, and M. Rebesco, *Geol. Soc. Spec. Publ.*, **276**, 95–110.
- Roberts, A. P. (1995), Magnetic properties of sedimentary greigite (Fe₃S₄), *Earth Planet. Sci. Lett.*, **134**, 227–236, doi:10.1016/0012-821X(95)00131-U.
- Roberts, A. P., and M. Winklhofer (2004), Why are geomagnetic excursions not always recorded in sediments? Constraints from post-depositional remanent magnetization lock-in modelling, *Earth Planet. Sci. Lett.*, **227**, 345–359, doi:10.1016/j.epsl.2004.07.040.
- Roberts, A. P., J. S. Stoner, and C. Richter (1999), Diagenetic magnetic enhancement of sapropels from the eastern Mediterranean Sea, *Mar. Geol.*, **153**, 103–116, doi:10.1016/S0025-3227(98)00087-5.
- Roberts, A. P., C. R. Pike, and K. L. Verosub (2000), First-order reversal curve diagrams: A new tool for characterizing the magnetic properties of natural samples, *J. Geophys. Res.*, **105**, 28,461–28,475, doi:10.1029/2000JB900326.
- Roberts, A. P., W.-T. Jiang, F. Florindo, C.-S. Horng, and C. Laj (2005), Assessing the timing of greigite formation and the reliability of the Upper Olduvai polarity transition record from the Crostolo River, Italy, *Geophys. Res. Lett.*, **32**, L05307, doi:10.1029/2004GL022137.
- Roberts, A. P., F. Florindo, J. C. Larrasoana, M. A. O'Regan, and X. Zhao (2010), Complex polarity pattern at the former Plio-Pleistocene global stratotype section at Vrica (Italy): Remagnetization by magnetic iron

- sulphides, *Earth Planet. Sci. Lett.*, 292, 98–111, doi:10.1016/j.epsl.2010.01.025.
- Roberts, A. P., L. Chang, C. J. Rowan, C.-S. Horng, and F. Florindo (2011), Magnetic properties of sedimentary greigite (Fe_3S_4): An update, *Rev. Geophys.*, 49, RG1002, doi:10.1029/2010RG000336.
- Rochette, P., G. Fillion, J.-L. Mattéi, and M. J. Dekkers (1990), Magnetic transition at 30–34 Kelvin in pyrrhotite: Insight into a widespread occurrence of this mineral in rocks, *Earth Planet. Sci. Lett.*, 98, 319–328, doi:10.1016/0012-821X(90)90034-U.
- Rowan, C. J., and A. P. Roberts (2005), Tectonic and geochronological implications of variably timed magnetizations carried by authigenic greigite in marine sediments from New Zealand, *Geology*, 33, 553–556, doi:10.1130/G21382.1.
- Rowan, C. J., and A. P. Roberts (2006), Magnetite dissolution, diachronous greigite formation, and secondary magnetizations from pyrite oxidation: Unravelling complex magnetizations in Neogene marine sediments from New Zealand, *Earth Planet. Sci. Lett.*, 241, 119–137, doi:10.1016/j.epsl.2005.10.017.
- Sachs, J. P., and R. F. Anderson (2005), Increased productivity in the subantarctic ocean during Heinrich events, *Nature*, 434, 1118–1121, doi:10.1038/nature03544.
- Sagnotti, L., P. Macri, A. Camerlenghi, and M. Rebesco (2001), Environmental magnetism of late Pleistocene sediments from the Pacific margin of the Antarctic Peninsula and interhemispheric correlation of climatic events, *Earth Planet. Sci. Lett.*, 192, 65–80, doi:10.1016/S0012-821X(01)00438-1.
- Sagnotti, L., A. P. Roberts, R. Weaver, K. L. Verosub, F. Florindo, C. R. Pike, T. Clayton, and G. S. Wilson (2005), Apparent magnetic polarity reversals due to remagnetization resulting from late diagenetic growth of greigite from siderite, *Geophys. J. Int.*, 160, 89–100, doi:10.1111/j.1365-246X.2005.02485.x.
- Stoner, J. S., J. E. T. Channell, and C. Hillaire-Marcel (1998), A 200 ka geomagnetic chronostratigraphy for the Labrador Sea: Indirect correlation of the sediment record to SPECMAP, *Earth Planet. Sci. Lett.*, 159, 165–181, doi:10.1016/S0012-821X(98)00069-7.
- Stoner, J. S., C. Laj, J. E. T. Channell, and C. Kissel (2002), South Atlantic and North Atlantic geomagnetic paleointensity stacks (0–80 ka): Implications for inter-hemispheric correlation, *Quat. Sci. Rev.*, 21, 1141–1151, doi:10.1016/S0277-3791(01)00136-6.
- Turner, J., S. R. Colwell, G. J. Marshall, T. A. Lachlan-Cope, A. M. Carleton, P. D. Jones, V. Lagun, P. A. Reid, and S. Iagovkina (2005), Antarctic climate change during the last 50 years, *Int. J. Climatol.*, 25, 279–294, doi:10.1002/joc.1130.
- Uenzelmann-Neben, G. (2006), Depositional patterns at drift 7, Antarctic Peninsula: Along-slope versus down-slope sediment transport as indicators for oceanic currents and climatic conditions, *Mar. Geol.*, 233, 49–62, doi:10.1016/j.margeo.2006.08.008.
- Venuti, A., and F. Florindo (2004), Magnetostratigraphy and environmental magnetism of two Quaternary deep-sea gravity cores from the west Pacific Southern Ocean, *Geochem. Geophys. Geosyst.*, 5, Q12011, doi:10.1029/2004GC000810.
- Villa, G., D. Persico, M. C. Bonci, R. G. Lucchi, C. Morigi, and M. Rebesco (2003), Biostratigraphic characterization and Quaternary microfossil palaeoecology in sediment drifts west of the Antarctic Peninsula—implications for cyclic glacial-interglacial deposition, *Palaeogeogr. Palaeoclimatol. Palaeoecol.*, 198, 237–263, doi:10.1016/S0031-0182(03)00403-6.
- Weeks, R., C. Laj, L. Endignoux, M. Fuller, A. Roberts, R. Manganne, E. Blanchard, and W. Goree (1993), Improvements in long-core measurement techniques: Applications in palaeomagnetism and palaeoceanography, *Geophys. J. Int.*, 114, 651–662, doi:10.1111/j.1365-246X.1993.tb06994.x.
- A. Caburlotto, Istituto Nazionale di Oceanografia e di Geofisica Sperimentale, Borgo Grotta Gigante 42/c, I-34010 Sgonico, Italy.
- A. Cavallo, F. Florindo, E. Strada, and A. Venuti, Istituto Nazionale di Geofisica e Vulcanologia, Via di Vigna Murata 605, I-00143 Roma, Italy. (fabio.florindo@ingv.it)
- C.-D. Hillenbrand, British Antarctic Survey, High Cross, Madingley Road, Cambridge CB3 0ET, UK.
- M. W. Hounslow, Lancaster Environment Centre, Lancaster University, Farrer Ave., Lancaster LA1 4YQ, UK.
- F. M. Talarico, Dipartimento di Scienze della Terra, Università di Siena, Via del Laterano 8, I-53100 Siena, Italy.